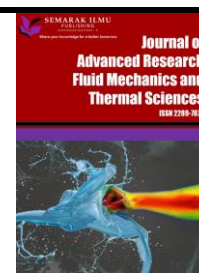




## Journal of Advanced Research in Fluid Mechanics and Thermal Sciences

Journal homepage:  
[https://semarakilmu.com.my/journals/index.php/fluid\\_mechanics\\_thermal\\_sciences/index](https://semarakilmu.com.my/journals/index.php/fluid_mechanics_thermal_sciences/index)  
ISSN: 2289-7879



# A Review on Non-Invasive Magnetic and Electric Field Excited Methods for Flow Characterisation of Incompressible Newtonian Low Conductive Liquids

Anusha Vadde<sup>1,\*</sup>, Govind Rangaswamy Kadambi<sup>1</sup>, Siddabasappa Channabasappa<sup>2</sup>

<sup>1</sup> Department of Electrical, Electronics, Communication Engineering, Faculty of Engineering, M. S. Ramaiah University of Applied Sciences, Bengaluru, 560058, Karnataka, India

<sup>2</sup> Department of Mathematics and Statistics, Faculty of Mathematical and Physical Sciences, M. S. Ramaiah University of Applied Sciences, Bengaluru, 560058, Karnataka, India

### ARTICLE INFO

#### Article history:

Received 30 May 2022

Received in revised form 22 October 2022

Accepted 5 November 2022

Available online 24 November 2022

#### Keywords:

Flow rate; Eddy currents; conductive fluids; Lorentz force; electric double layer

### ABSTRACT

Monitoring the flow rate of low conductive fluid is critical in sectors such as waste, culinary, chemical, pharmaceutical, oil and gas, and power. The flow meter can be used to measure several parameters like flow rate range, fluid electrical conductivity, cost and the scenario of desired monitoring. The existing invasive flow sensors for monitoring the velocity of conductive fluid are often associated with undesirable attributes of being obstructive, prone to interference effects, corrosion, significant pressure reduction, and energy loss in pipe systems causing severe and long-term damage to pipes during installation. This paper presents a comprehensive survey of various non-invasive methods for characterizing low conductive fluid flow based on the sources of strong magnetic and electric fields. This review discusses fundamental insights for understanding the physical phenomenon in the generation of eddy currents, Lorentz force, and the formation of the electric double layer with pertinent illustrations and discussions. The review presented in this paper concludes that each non-invasive measurement technique has limitations based on the excitation source of either magnetic or electric fields. Different values of low conductivity of fluid flow and flow velocity have been considered in various studies to get an in-depth understanding of the capability of selected techniques so that their scope and versatility can be researched further. This paper also highlights that emerging technologies like cryostats with superconducting magnet systems, which unquestionably exceed the mass limitation, have become viable in applications such as Lorentz force velocimetry.

## 1. Introduction

Flow rate measurement is imperative in numerous fields such as Pharmaceutical and Chemical industries, agriculture, food processing, and bio-medical, contributing to countries' economic growth. Various researchers are still making numerous efforts to design and develop novel and modified flow measurement techniques for sustainable industrialization. Emerging innovation in

\* Corresponding author.

E-mail address: [vaddeanusha203@gmail.com](mailto:vaddeanusha203@gmail.com)

<https://doi.org/10.37934/arfmts.101.1.90120>

fluid flow measurement techniques enhances the economic viability and adaptability of the usage of measuring instruments. Monitoring conductive fluid flow velocity is critical in the waste, culinary, pharmaceutical, oil and gas, chemical and power sectors. The choice of flow meter used to measure conductive liquid flow depends on several parameters, including flow rate range, the conductivity of the liquid, cost, and application area. Measuring the flow rate of fluid through flow meters is a challenging task. Installation flaws can impair measurement accuracy even when noise, vibration, and dirt problems are considered. The accuracy of flow measurement for industrial applications is between 0.2 % and 5% of its Full-Scale Range (FSR). However, when measuring a conducting liquid's flow, the electromagnetic flow-measurement technique is significantly more accessible and less expensive than other methods such as absorption type, turbine type, Coriolis force type, target type, vortex type, and many other types [1-4]. Electromagnetic flowmeters are commonly used in process industries to measure the volume flow rate of a conducting liquid, as this technology is accessible compared to other methods. In an electromagnetic flow meter, coils connected to an Alternating Current (AC) or Direct Current (DC) source produce an intense magnetic field in the specified region of the flow tube. Inside the tube, two sensing electrodes are arranged diametrically opposite each other in contact with the conductive liquid. The electric potential between the electrodes is directly proportional to the velocity of fluid flow [5,6]. Even though several electromagnetic flow meter designs have emerged during the last century, they are associated with limitations such as electromagnetic interference effects, fluctuations in supply voltage, corrosion of electrodes, and electrical contact with the conductive fluid flow, which is necessary to measure the potential difference. However, installing such an electromagnetic flow meter is intrusive because it requires stopping the process and inserting it in the pipeline. Non-contact flow meters which are functionally applicable to low conductive fluids in chemicals, food, drinks, blood, and aqueous solutions in the pharmaceutical sectors are necessary to overcome the issues of contact-based flow meters. Non-invasive flow monitoring through opaque walls or in opaque liquids would be quite beneficial [7-10]. Numerous practical devices, such as non-obstructed probes, non-invasive sensors or transducers, are designed to serve as part of Measuring Instruments (MIs) or systems to detect changes in the fluid flow of charged particles. The focus of this paper is on incompressible Newtonian fluids. The main contributions of this paper are as follows

- i. To present a basic overview of the non-invasive method for measuring the flow rate of fluids.
- ii. To discuss the assumptions for the installation of a non-invasive type of flowmeter.
- iii. To enumerate the fundamental concepts involved in the various techniques for monitoring the conductive fluid flows.
- iv. To emphasize the significant contributions of non-invasive flow metering techniques in measuring the flow rate of low conductive fluids.

Concluding remarks and hopeful anticipation in developing non-invasive methods for measuring the flow rate in various industrial applications are also presented in this paper.

## **2. Non-Invasive Method**

The term "Non-contact/Non-Invasive flowmeter" refers to a device that does not physically contact the liquid being measured or with the pipe wall through which the fluid flows. Such flowmeters are very useful in glass making and metallurgy, where the pipe walls are heated well over 1000°C. Non-Contact (NC) flowmeters are beneficial when walls are contaminated, such as in

processing radioactive chemicals, when pipes are vigorously vibrating, or when portable flowmeters must be made commercially available. In an invasive method, sensing elements that come into contact with the fluid are susceptible to damage and contamination from the fluid, which can reduce the life of the flow meter. During the process of installing or removing them, there is a possibility that the fluid may leak and that the pipe fittings may be damaged [11].

Additionally, since the placement of the flowmeter is within the pipe, the flow rate can only be measured in specific locations. Consequently, fluid flow is disturbed within the pipe resulting in a pressure drop and an increase in energy loss. In these circumstances, non-invasive measurement (which overcomes the limitations of invasive flowmeters) of fluid flow in a pipe exhibits enhanced appeal. Non-invasive flow meters are classified into two types as shown in Figure 1. In the intrusive type, the sensor is in contact with the fluid flow even though it disturbs the flow, as shown in Figure 1(a). In a non-intrusive flow meter, the sensor placement does not disturb the fluid flow, as in Figure 1(b). For accurate flow measurement, the type of fluid whose flow rate is to be measured determines the selection of flow measuring method [12]. The physical location of a flow meter can impact the precision of measurement.

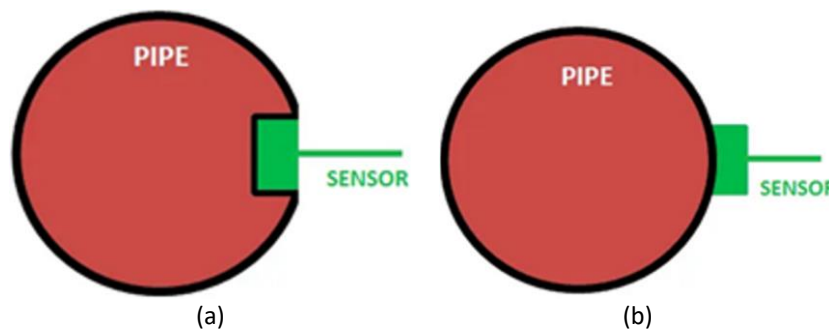


**Fig. 1.** Type of Non-Invasive measurements [12]; (a) intrusive, (b) non-intrusive

Measuring the flow rate of fluids often requires the knowledge of the quantitative value of fluid in and out of a pipe. The flow rate can be expressed as fluid velocity, volumetric flow rate, and mass flow rate. The mass flow rate is generally measured for "energy-giving fluids" such as gasoline and natural gas. For low-conductive fluids such as water and electrolytic solutions, volumetric flow rate or velocity is a measurable quantity. Volumetric flow rate,  $Q$  is defined as the "volume of fluid that passes through a given surface per unit time" as given in Eq. (1) [13].

$$Q = \frac{V}{t} = \frac{A \cdot l}{t} = A \cdot v = \frac{\pi}{4} D^2 \times v, \quad (1)$$

where  $V$  is duct's volume,  $A$  is duct's area,  $v$  is the flow velocity in m/s,  $t$  is time in s,  $l$  is the duct's length in mm or m, and  $D$  is the inner diameter of the duct.

### 2.1 Assumptions in Measurement of Fluid Flow in Pipe

Fluid flow in pipes is an extremely complicated phenomenon; hence, its modelling is restricted to near-ideal situations. Various factors influence the behaviour of specific fluid flow and are frequently interrelated. As a result, it is required to impose constraints that simplify the fluid dynamics model by only considering relevant conditions for the design of non-invasive fluid flow measurement in applications such as agricultural, metal, and food processing industries. Even though the following

factors are not constant for all expected conditions, they do not affect the fluid flow characterization [14]

- i. Internal flows are fluids that are confined by solid surfaces.
- ii. The pipes can only hold one fluid (i.e. water or electrolyte solutions or insulating liquids). There are no air bubbles, ice, or significant dissolved particles in the water flow.
- iii. Water's physical characteristics, such as kinematic viscosity and density, are affected by its temperature. These can be assumed to be constant at all temperatures for the specified temperature ranges.
- iv. The density of the fluid does not change with the pressure.
- v. The velocity in the flow channel/duct/pipe and hydrodynamic characteristics of the flow do not change from point to point at any instant.
- vi. The pipe's internal roughness is a variable that might change over time as the pipe erodes or sediment accumulates on the inside surface. The configuration of upstream and downstream of the duct is not consistent and changes significantly between installations, depending on the physical constraints of the surrounding area.

### **3. Applications of Magnetic Field as Source of Excitation: Theory And Working Principle**

Industries emphasize non-invasive methods implemented on the outer cylindrical surface to avoid the disturbance of fluid flow and abstain from closing down systems for installations. Researchers have shown keen interest in the non-invasive methods using the input source as magnetic and electric fields since conductive fluid flow is within the duct.

Flow has been measured with the source of magnetic fields for a long time. Walmsley and Woodford [15] suggested the analytical and numerical approach of the electric current induced by the laminar flow of a low conductive liquid using a non- equilibrium boundary condition. When Michael Faraday attempted to measure the Thames River's velocity in 1832, it sparked a scientific revolution. The inductive flowmeter is a thriving commercial use of Faraday's technique that involves subjecting a flow to a magnetic field and measuring the induced voltage using two electrodes. The ElectroMagnetic Flowmeter (EMF) is a device that utilizes "Faraday's law of electromagnetic induction" to measure the flow rate by detecting the generated voltage across the metal electrodes when fluid flows through an intense magnetic field. Although inductive flowmeters are commonly used for measuring the flow of low-temperature fluids such as beverages, chemicals, and wastewater, they are unsuitable for measuring the flow of metals. Due to the insertion of electrodes into the fluid, utility of EMF is restricted to applications at temperatures much below the melting points of practically essential metals.

In a conventional EMF, an electrode made of metal is inserted through the wall thickness of the measurement tube to collect the induction signal, as shown in Figure 2.

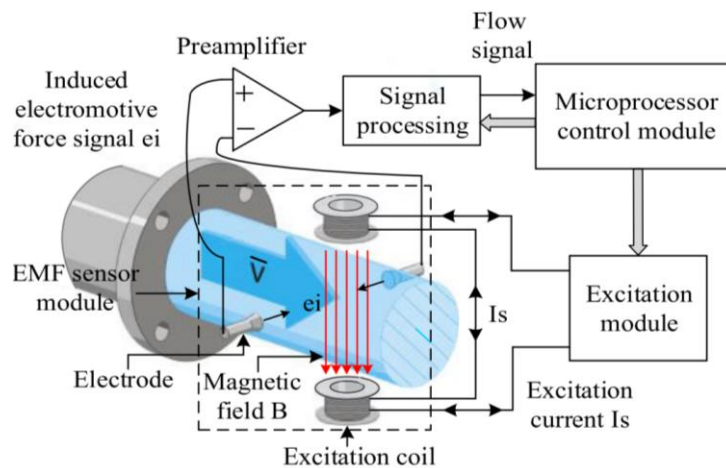


Fig. 2. Electromagnetic flow meter [22]

The induced electromotive force  $e_i$  is produced when fluid with an average velocity  $v$  cuts magnetic field line  $B$  and  $e_i = kBDv$ . Where  $k$  is the constant, and  $D$  is the inner diameter of the measurement pipe. Till now, it is observed that the fluid motion induces magnetic and electric fields when an external magnetic field is applied. Stefani and Gerbeth [16] discussed measuring fields at the wall of the duct and outside the fluid volume and the reconstruction of the flow velocity from measured fields using Tikhonov regularisation. Hussain and Baker [17] proposed that the segmented electrodes placed in the new EMF design results in a non-contact flow meter. A dielectric layer separates the electrode from the fluid. The thinnest possible dielectric layer is employed. Based on the thickness of the dielectric, required potentials are observed. While constructing the flow meter, the stepped electrode is switched with smooth electrodes. The second layer of insulation surrounds the electrode, and a shielding electrode is placed outside of duct's surface and driven by a voltage-follower circuit. The dielectric material (that sufficiently covers the electrodes) prevents microphonic effects and its relative permittivity must be so chosen to lower the internal impedance of the flow meter. The exterior insulator must be durable; therefore, a relatively low permittivity value is selected. The full-scale measurement of zero drift was 0.2%. During the casting process for the electrode structure, a slight distortion resulting from the contraction of the epoxy resin results in a higher relative permittivity value than the desired value. The electrode is easily contaminated when measuring viscous substances, which impacts the measurement outcomes. Sakurai and Ishihara [18] discussed the measurement method of capacitive EMF as shown in Figure 3, which successfully addresses the contamination issue and may achieve long-term maintenance-free operation. In this method, an electrode is placed outside the measuring tube wall and does not make direct contact with the fluid being measured.

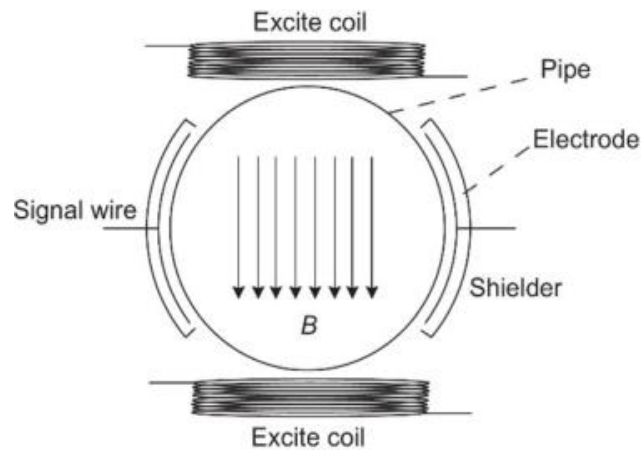


Fig. 3. Capacitive electromagnetic flow meter [18]

Two challenges must be considered to ensure the quality of the acquired voltage signal. They are a weak signal at the source and a high impedance at the source. Increasing the driving current and the number of turns of the excitation coil will result in a stronger magnetic field being applied to the measuring tube, thereby enhancing the amplitude of voltage signal. However, the increase in number of turns of coil and wire diameter results in a larger volume of excitation coil, which is not ideal for space-constrained conditions. Because it is challenging to improve signal strength considerably, a viable option is to avoid signal loss during signal acquisition [19]. The main element influencing the effectiveness of signal acquisition is the source impedance of voltage signal, which is influenced by capacitance and the frequency of excitation signal. The lower source impedance is advantageous for signal acquisition; it may be attained by increasing source capacitance and employing a higher excitation frequency. Enhancing the area of the detection electrode, a tube material with a high dielectric constant, and decreasing the wall thickness of the tube are the typical methods for increasing the coupling capacitance [19].

### 3.1 Excitation Frequency

Many research studies are focused on increasing the frequency of excitation signals to improve the output signal detected by the sensors. The high frequency is chosen when the process is chaotic with slurries, or flow rates fluctuate quickly. The low frequency is chosen when the flow rate is slow or the fluid flow ceases and monitoring of the fluid flow is not required continuously.

Dual frequency excitation is catalogued into two classes; complicated dual frequency and time division dual frequency excitation. Time division dual frequency excitation improves the zero-point stability of the flow meter and also the dynamic responsiveness to rapid changes in flow velocity. The resistance to low-frequency noise is also increased [20,21]. Theoretically, while the components of high-frequency excitation are used to improve the dynamic response capability, the low-frequency excitation component is used to assure zero-point stability.

The frequency excitation waveforms with time division dual frequency excitation is shown in Figure 4(a). Low-frequency excitation cycles and high-frequency excitation cycles form one excitation cycle. The high-frequency simulation cycles occur alternately with the low-frequency cycles. The low-frequency and high-frequency components each have their frequency range, which can be chosen independently. For example, for an excitation frequency of 50Hz, 6.25Hz can be chosen for the low frequency, and 25Hz to 75Hz can be chosen for the high frequency. Figure 4(b) shows that the numerous sensor signals are sampled during the low-frequency excitation period to capture the signal's evolving pattern from when the excitation current direction is reversed until the magnetic

field is assumed to be stable. During the periods of high-frequency simulation, the sampled data is utilized to enhance the zero-point stability of the system [21].

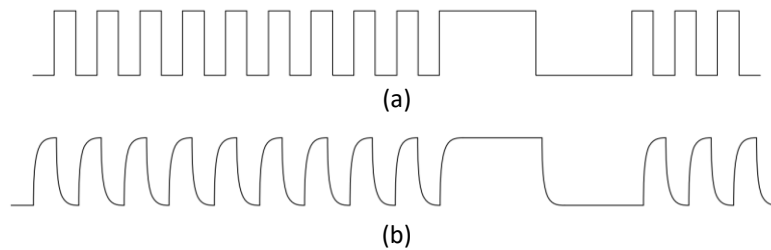


**Fig. 4.** Square wave frequency excitation waveforms [20]; (a) input signal, (b) output signal

### 3.2 Role of $\nabla \times E = -\frac{\partial B}{\partial t}$

The excitation frequency is enhanced by the step excitation technology, which improves the equivalent excitation frequency without increasing the rise time of the excitation current. Thus, it reduces the slurry noise in the acquired voltage signal at the electrodes.

In the EMF measuring method shown in Figure 5,  $-v \times B$  of the “circuit” moves under constant excitation and is used to calculate the induced potential proportional to the fluid velocity,  $v$ . The  $\nabla \times E = -\frac{\partial B}{\partial t}$  corresponds to “field alterations” at the constant switching excitation, where  $\nabla \times$  is a curl operator,  $\frac{\partial B}{\partial t}$  is the rate of change in magnetic field, and  $E$  is the vortex electric field, as shown in Figure 5(b). The strength of the vortex electric field during the excitation-switching process increases with increasing  $\frac{\partial B}{\partial t}$ . The primary technique to raise  $\frac{\partial B}{\partial t}$  while maintaining the same liquid characteristics is to increase the rate of change in excitation current in the coil as shown in Figure 5(a). Since the coil is an inductive load, high-voltage excitation is frequently utilized to boost the rising rate of excitation current. After switching the excitation,  $\frac{\partial B}{\partial t}$  goes to zero in the constant excitation. During the interval of  $\frac{\partial B}{\partial t} = 0$ , the moving charge experiences the Lorentz force and separates the positive and negative charges accumulated at the electrodes. The interference charges can be pushed away from the electrode surface because the magnitude of  $\frac{\partial B}{\partial t}$  is significantly larger than  $v$ , since the vortex electric field force is much stronger than the Lorentz force. The shorter the time gap between the two  $\frac{\partial B}{\partial t}$  values, lower the possibility that solid particles striking the electrode results in slurry noise interfering with the electrode signal [22].

AC electromagnetic flowmeters provide a low alternating voltage with high electromagnetic interference. In most cases, the coils that produce the driving magnetic field interfere strongly with the input signal, which has a magnitude of less than 1 mV. A trapezoidal magnetic field confines the magnetic interference to the transitions between field values, which afterwards enables the detecting voltage during the flat intervals of magnetic field. The voltage detected by the electrodes has to be amplified and demodulated to retrieve the voltage proportionate to the average fluid velocity. An AC-coupled amplifier rejects electrochemical potential from electrodes. A differential amplifier is used for the amplification of the signal. Synchronous rectification and sampling with zero-order hold are the first two steps in the demodulation process, which is then followed by low-pass filtering. An improvised method of signal acquisition circuit and associated signal processing technique are discussed in the study by Li *et al.*, [22]. The rotating capacitor filter is a way to process

signals that are based on the technology of phase-sensitive detection; it can separate the weak signal from the intense and wide-band background noise. The bootstrap amplifier circuit is a preamplifier to pick up signals from two electrodes. An instrument amplifier is used for further amplification of the signal. Although shielding procedures are employed, the signals received by the signal-detecting circuit of EMF are unavoidably intermingled with various forms of noise because it operates in an environment with complex and intense electromagnetic interference. The signals are differentially amplified to remove the common mode interference before being passed to a rotating capacitor filter to remove any residual noise.

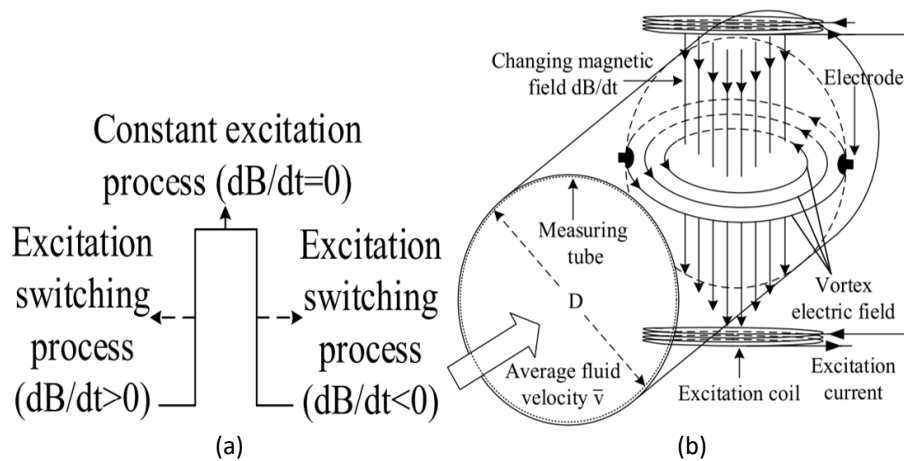


**Fig. 5.** Schematic diagram of flow meter [22]; (a) Proces of excitation, (b) Electric field in form of vortex

The literature reveals that the capacitance electromagnetic flow meter is intrusive, and improvised technologies have been used to improve the frequency excitation system and remove the residual noise in the signal. An extensive magnetic system must be used to obtain better resolution in velocity measurements. The Lorentz force concept has been introduced for enhancing the resolution of conductive fluid flow velocity by the flow measurement system.

### 3.3 Lorentz Force

The magnetic field is generated in two distinct ways: one uses group of current-carrying coils, and the second one involves placing a strong permanent magnet. The conductive fluid flows through the generated magnetic field, inducing the eddy currents. The direction of the magnetic field varies based on the placement of the magnetic system, as shown in Figure 6. Based on the flux direction in the conductive fluid flow, flow meters are classified as Longitudinal flux flow meters and Transverse flux flow meters.

In Longitudinal flux flowmeters, the magnetic field is axisymmetric. The axis of symmetry of magnetic field aligns with the axis of the duct as shown in Figure 6(a). In Figure 6(b), the magnetic field is transverse to the fluid flow in the duct and the magnet system is placed on one side of duct. Longitudinal flux flowmeters circumferentially encircle the duct. They need not be dismantled and reassembled for use in different places. This class of flow meter is generally used for high-conductive fluid flows. Induced eddy currents lead to Lorentz force, which separates the charges in conducting fluid flow. By Newton's third law, the developed Lorentz force acts opposite to the source generating a magnetic field [23]. The Lorentz force scaling behaviour is expressed in Eq. (2).



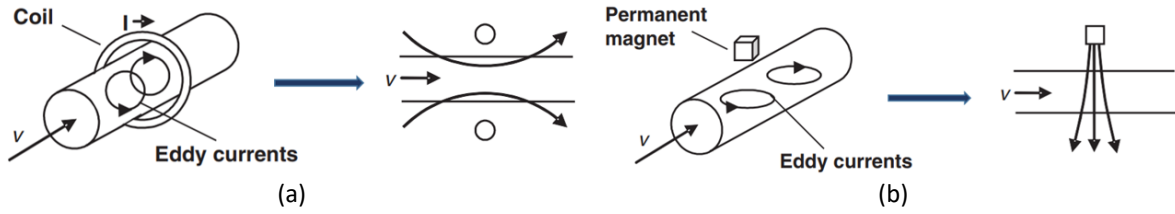


**Fig. 6.** Schematic view of the direction of magnetic field [23]; (a) Longitudinal Flux, (b) Transverse Flux

$$F_{\text{lorentz}} = \sigma \times v \times B^2 \quad (2)$$

Where  $\sigma$  is electrical conductivity,  $v$  is the mean velocity of the fluid in the duct (channel) and  $B$  is the magnetic flux density.

The primary magnetic field,  $B$  is produced by the permanent magnet, exemplified by the spatial distribution of magnetization density, as shown in Figure 7(a). The primary magnetic field is responsible for the primary currents in the closed channel. When a steady electrically conducting fluid flow is subjected to a primary magnetic field, the secondary currents (or) eddy currents are produced in the fluid flow as shown in Figure 7(b). According to Ohm's law, the current density induced in the conductive fluid flow is defined in Eq. (3).

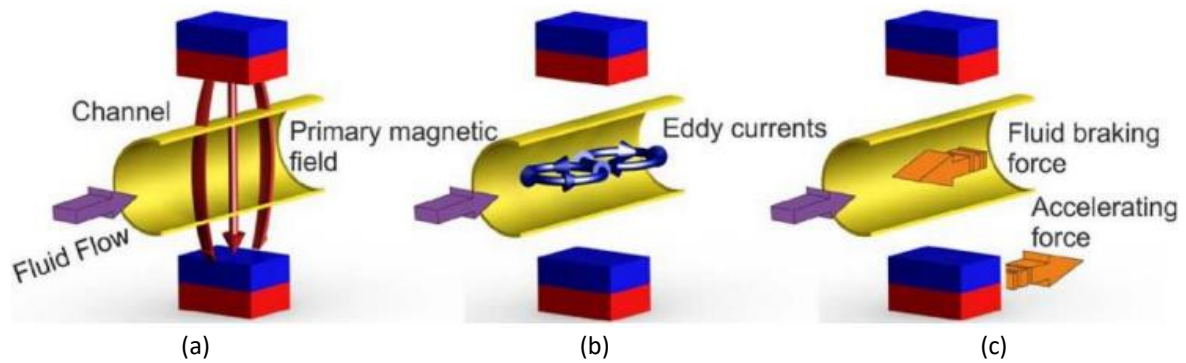


**Fig. 7.** Schematic view of the generation of Lorentz force in fluid flow [24]; (a) Induction of primary magnetic field, (b) Generation of eddy currents, (c) Braking force on fluid flow

$$j = \sigma(v \times B - \nabla\varphi) \quad (3)$$

where  $\sigma$  is the fluid's electrical conductivity,  $j$  is current density due to secondary currents, and  $\varphi$  stands for the electric scalar potential. The eddy current's interaction with the primary magnetic field causes a Lorentz force as defined in Eq. (4), which opposes the fluid flow in the channel, as shown in Figure 7(c).

$$F_f = \int j \times B d^3r \quad (4)$$

The secondary currents in turn, generate the secondary magnetic field,  $b$ . From Biot-Savart's law,  $b$  over the volume within the duct at a position  $r$  given by Eq. (5).

$$b(r) = \frac{\mu_0\sigma}{4\pi} \iiint [V(r') \times B(r')] \times \frac{r-r'}{|r-r'|^3} dV' - \frac{\mu_0\sigma}{4\pi} \oint_S \varphi(s')n(s') \times \frac{r-s'}{|r-s'|^3} dS' \quad (5)$$

where,  $dV'$  signifies the volume element and the position vector  $r'$ . The surface integral signifies a  $dS'$  surface element, and  $n(s')$  denotes the average vector at the position  $s'$  of the duct surface. The interaction of the secondary magnetic field with primary currents, in turn generates the Kelvin force (i.e., Lorentz force) as defined in Eq. (6), which acts on the permanent magnets (magnet system).

$$F_m = \int J \times b d^3r \quad (6)$$

From the principle of reciprocity, Eq. (4) and Eq. (6) are related by Eq. (7).

$$F_m = -F_f \quad (7)$$

Hence, Eq. (7) is the relation between the two forces responsible for Lorentz Force Velocimetry (LFV). Thus, it is suffice to state that the magnetic system serves as a source of the primary field and a sensor of the secondary field. Consequently, when the magnetic field strength increases, then the sensitivity of a measuring system also improves. A Lorentz force flowmeter is a device that calculates the flow rate by measuring Lorentz force. There are two distinct techniques to develop a Lorentz force flowmeter. They can be constructed as static flowmeters in which the magnet system is at rest and the force acting on it is measured [24]. Alternately, they can be configured as rotary flowmeters in which the magnets are positioned on a revolving wheel, and the velocity of the wheel's rotation is a measurement of the flow velocity.

A susceptible pendulum force measurement device based on the deflection principle has been successfully used to demonstrate the viability of LFV for flow rate measurements of low conducting electrolytes. According to the research by Thess *et al.*, [23], the Lorentz forces produced by the fluid flow are directly related to the fluid's conductivity. However, the conductivity of electrolytes is only 1 S/m, while that of molten metals is on a scale of  $10^6$  S/m. Therefore, the LFV force on electrolyte flows is in micronewtons, or  $10^6$  times less than the LFV force on molten metal flows. Despite the challenges associated with force resolution, LFV can be used to characterize electrolyte flows. The fluid and the magnet experience Lorentz force when a magnet system is placed close to a moving conducting fluid [24]. If the magnet system is freely suspended, the force will displace the magnet system. In the configuration presented, the suspension is provided by parallel tungsten wires. An active force causes a parallel displacement of the coupling element associated with the fixed support, independent of the location of the force application. A corner cube interferometer is used to determine the displacement of the coupling element. Wegfrass *et al.*, [25] deployed a powerful magnet system with a 1 mm air gap on both sides of the test section to create a high magnetic field intensity. The magnet system had two NdFeB high-energy magnets of grade N48 to produce the highest possible magnetic flux density. Thin tungsten wires resembling a pendulum hold the magnet system itself, as illustrated in Figure 8. The complete measuring system was mounted on a granite block and encased in a sand-filled box to minimize the impact of ambient building vibrations.

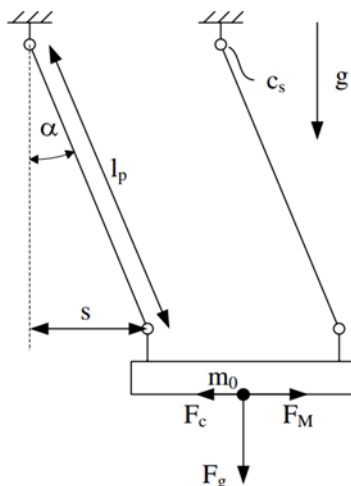


**Fig. 8.** Schematic view of pendulum force measurement [25]

The pendulum's deflection,  $s$  is measured by an interferometer as shown in Figure 8. Considering the pendulum's stiffness  $K_s$ , which is often specified as the calibration factor of the system, Lorentz force  $F_L = sK_s$ , is developed by the amount of deflection from the zero point. The flow-induced Lorentz force,  $F_M$  causes a parallel deflection  $s$  of the coupling element to the aluminium frame. A susceptible pendulum force measurement system that uses the idea of deflection has effectively proved the viability of LFV for flow rate measurements of low conducting electrolytes. After calibrating, the stiffness of the measurement system was somewhat similar to the numerical method. The measuring equipment had been calibrated, and its rigidity was closely matching with that to numerical simulation. The sensitivity of measurement system was computed for various values of velocity and various electrical conductivities of 2.3 S/m, 6.5 S/m, 8.5 S/m, 13 S/m and 14 S/m as shown in Figure 9.

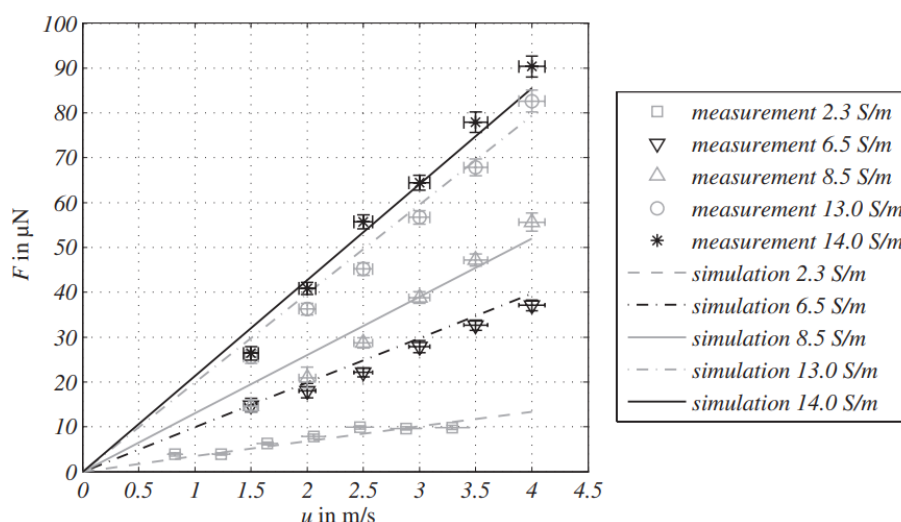


**Fig. 9.** Sensitivity characteristics of Lorentz Force Velocitymetry [25]

In order to overcome the suspension of a huge mass of magnet system, Werner *et al.*, [26] enumerate the process of designing the magnetic system for a LFV with electrical conductivity of glass metals (10 S/m). Werner *et al.*, proposed the idea of a reduction in mass of the magnet system (which is hanging) on the force measurement unit. In electrically stimulated magnetic systems, the

coil is attached to the ground, while the iron yoke, which interacts with the fluid, passes through it with a tiny air gap between it and the inner wall of the coil. This air gap is required to detect a minimum yoke deflection generated by the Lorentz force.

Investigations have been carried out to develop a mechanism to detect the Lorentz force to balance the electromagnetic force compensation. This will allow for a higher resolution of the forces that are being detected. Vasilyan and Froehlich [27] discussed the Lorentz force detection system to balance with the so-called Electromagnetic Force Compensation (EMFC), allowing much more improved force resolution. Lorentz force is induced in the turbulent flow of saline water inside a glass duct with the interaction of the transverse magnetic field. The magnet system comprised two identical permanent magnets that are magnetically coupled and fixed on an aluminium frame at a distance of 32 mm from the duct and a free oscillatory pendulum as shown in Figure 10. This arrangement allowed a minimum air gap of 1 mm on either side of the glass duct.

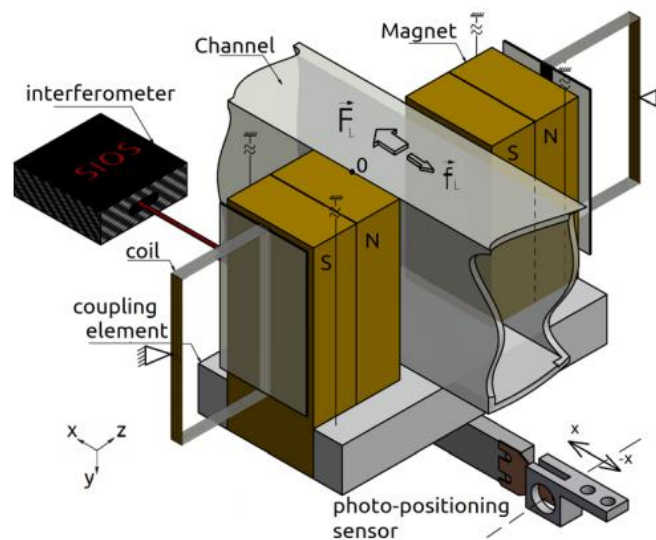


**Fig. 10.** Electromagnetic force compensation system [27]

Magnet will have a deflection due to the Lorentz force acting on it. An optoelectronic position sensor has been used to measure the position of magnet system, as shown in Figure 10. This sensor consists of a Light Emitting Diode (LED) oriented toward a differential photodiode with both optical axes blocked by a rectangular aperture mask and securely fastened to the magnet system to ensure the effective deflection is exerted proportionately on the sensor output. The converted voltage signal is sent to Digital Proportional Integral Differential (PID) controller, which generates a compensatory current in a current-carrying conductor which is in close proximity of magnets. This ensures that the aperture maintains its zero-balance position by applying an electromagnetic force between the magnet system and wires. The proposed measurement system also overcomes gravimetric uncertainties by balancing the pendulum's position. Instead of enhancing the resolution of measured force, controlling the position based on the zero point provides the added benefit of reducing the non-linear impacts present across the whole measurement range of the positioning sensor. Halbedel *et al.*, [28] discussed the higher-precision (state-of-the-art) commercially available weight cells used to present more exact and accurate flow data. An EMFC method with a linear voice coil was used to bring the proportional lever arm to the point of zero. Vasilyan *et al.*, [29] discussed the force measurement system for enhancing the performance of LFV. The proposed measurement system increased the resolution of force by the order of 2 depending on the equalization of zero point employing EMFC. A novel differential force measurement system with two identical EMFCs has been

designed for the measurement of horizontal forces, specifically to correct for the vibrational and tilt effects. The first EMFC contains the magnet structure and is meant to measure the Lorentz force. In contrast, other EMFC contains an equivalent dead weight composed of a non-ferromagnetic substance (copper), whose diamagnetism is minimal compared to the ferromagnetism of permanent magnet.

More research studies are required before commercializing EMFC LFV technology, particularly for electrolytic flows where conductivity values are low and obtained Lorentz forces are on the scale of some  $\mu\text{N}$ . With the use of permanent magnets, the magnetic flux, which is perpendicular to the direction of the channel (duct), forms a wide, dispersed flux surrounding the channel, leading to an enormous magnetic resistance. Effective magnetic flux density drops in the interaction zone. Typically, an iron yoke is employed to lower the magnetic resistance and direct the magnetic flux between two magnets with minimal losses. In recent years, it has been demonstrated that due to stringent weight constraints, an iron yoke is less effective than a lightweight, non-magnetic fixture. A specific combination of Halbach arrays are introduced in the research by Vasilyan *et al.*, [29] to prevent the large spread of magnetic field thereby decreasing the impact of adjacent ferromagnetic materials. NdFeB grade N52 material is used for the analysis.

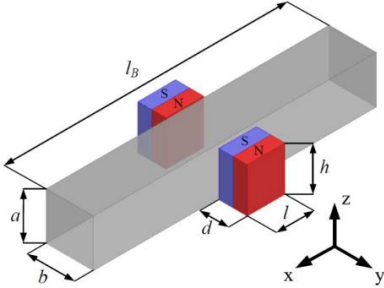
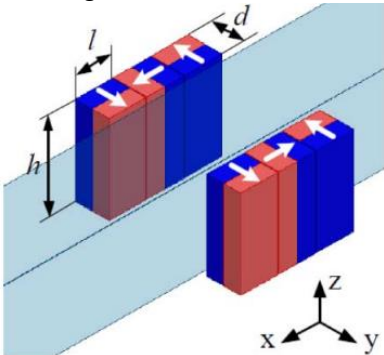
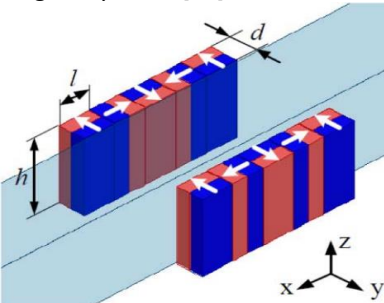
Choi and Yoo [30] introduced the concept of combining Halbach arrays with the cladding method to improve existing magnet systems significantly. Magnet systems are optimized geometrically based on a physical basis using finite element simulations. Werner and Halbedel [31] discussed the optimization of a conventional magnetic system for the velocity measurement of electrolytes using LFV. The various magnet designs and their dimensions are listed in Table 1. The obtained Lorentz force is numerically evaluated using an appropriate boundary condition assigned to the developed model in COMSOL – MATLAB environment. The length of the magnet (in stream wise direction) and height (perpendicular to the flow that is parallel to channel (duct) walls) are the free parameters for optimization. Due to the restricted mass of 950 g, the thickness of the magnet (perpendicular to the channel walls) is the output. Magnets with identical geometries are arranged on either side of the channel and magnetized perpendicular to the orientation of the channel wall. The conventional magnet system as shown in Figure 11 is replaced with the two arrays of the Halbach magnet system with the same mass as listed in Table 1. Two arrays of Halbach patterns face one another to increase the strength of the magnetic field. Two arrays of three and five Halbach patterns are shown in Figure 12 and Figure 13 to increase the Lorentz force for the low conductive fluids.

Choi and Yoo [32] investigated the feasibility of optimizing the magnetization patterns of these arrays for fixed geometries in eddy current braking applications and the most significant repulsion/attraction forces between the two magnet arrays. The Halbach array is promising for LFV applications with maximum attraction forces based on Choi's findings. Choi *et al.*, presented the Halbach magnet array system for LFV to increase the Lorentz force ( $F_L$ ). The Halbach magnet system reduces the external stray magnetic field and directs it into the inside of magnets; hence the maximum magnetic field penetrates into a flow channel. The arrangement of the Halbach magnet array is shown in Figure 14. The magnet is divided into ten rectangular bars, with five on each side of two blocks opposite to each other.

Apart from the Halbach magnet array, Fröhlich *et al.*, [33] also concentrated on the gravity forces, which indirectly affect the Lorentz force ( $F_L$ ). Hence, a system called Electromagnetic Force Compensation weighing balance was developed. It was placed inside the supporting setup frame and on 800 kg granite stone. Detecting minuscule Lorentz force in the test channel's noisy surroundings is challenging for low-conductive fluids. The newest Electromagnetic Force Compensation (EFC) balance method is used for the Lorentz force measurements. This method limits the mass of the permanent magnet to approximately 1 kg, which is responsible for the generation of Lorentz force.

This method limits the Lorentz force to the order of  $\mu\text{N}$ , despite the numerical refinements of the magnet's shape and rare-earth high-field magnet systems resulting in limits on the electrical conductivity of the fluid.

**Table 1**  
 Various magnet system designs

Magnet Design	Dimensions ( $l \times h \times d$ ) mm	Lorentz force
 <p><b>Fig. 11.</b> Conventional Magnet System [31]</p>	38.5 × 51.9 × 31.7	35 $\mu\text{N}$
<p>A perfect magnetic conductor has been placed on the backside of the north pole of the right side magnet as well as the south pole of left side magnet</p>  <p><b>Fig. 12.</b> Two arrays of three Halbach magnet systems [31]</p>	49.2 × 59.5 × 21.6	54 $\mu\text{N}$
 <p><b>Fig. 13.</b> Two arrays of five Halbach magnet systems [31]</p>	21.2 × 51.4 × 19.4	76.7 $\mu\text{N}$
	Optimized × Optimized × 19.4	101. $\mu\text{N}$ and Obtained saturation force is approximately 115 $\mu\text{N}$

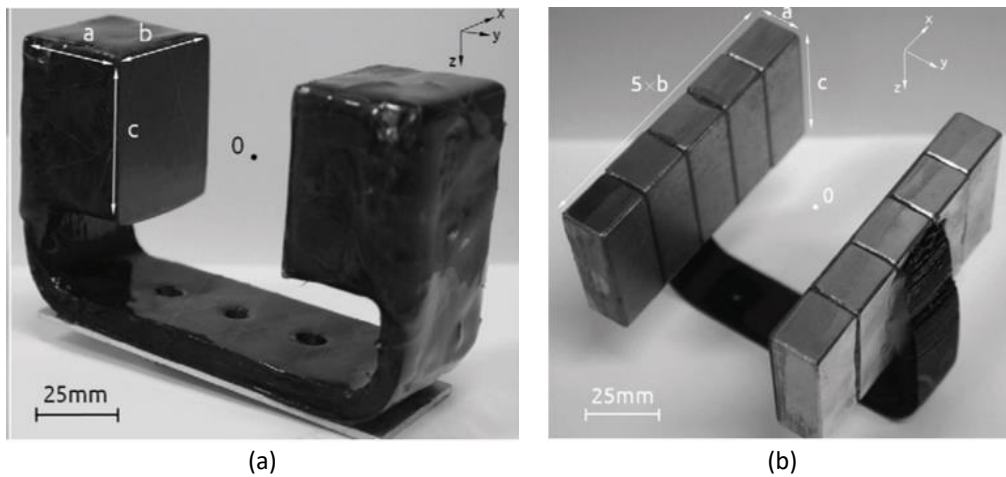


**Fig. 14.** Magnetic system designs [28,32]; (a) Permanent magnet, (b) Halbach array

Consequently, it limits the resolution of measurement of force. Larger magnet systems are employed to improve the resolution in obtained signals. However, it is impossible to employ larger magnet systems without compensating the vertical acting force. Resagk and Ebert [34] discussed the Buoyancy-based Weight Force Compensation (WFC) method in 2015 for enhancing the resolution of signals at higher velocities. By this method, the mass of the magnet system is enhanced to 3.01 Kg. Paraffin oil and water are considered low conductive media in the tank to prevent interference with Lorentz force measurement systems. A variation of about 5.6% between the measurement of water with reference value is depicted in Figure 15.

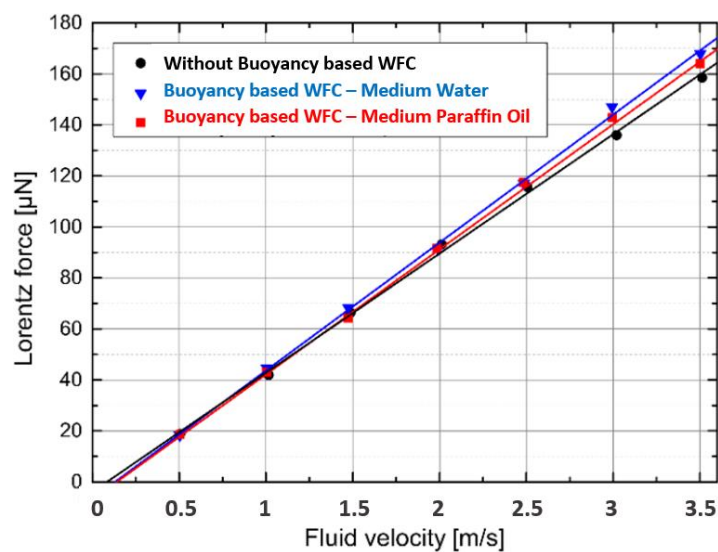


**Fig. 15.** Variation in flow velocity using Buoyancy-based WFC flow meter [34]

There is no detrimental impact on precision measurement due to the dampening of force amplitudes or increased noise levels. There is no variation in amplitude, and the moving average filter can remove any additional noise. As a result, this approach can enhance the resolution of Lorentz force velocimetry by at least a factor of three. In general, there are no restrictions on employing Halbach magnet arrays with 10 kg of weight to achieve a rise in resolvable fluid velocity or a reduction in the electrical conductivity of fluid by a factor of 10.

The bulk High-Temperature Superconducting (HTS) magnet, unlike PMs, has the distinctive ability to produce a conically shaped magnetic flux density ( $B$ ) distribution with a strong flux gradient. The

HTS can produce a magnetic field significantly more substantial than the NdFeB permanent magnet with the same mass. Two Y-Ba-Cu-O samples are used in the HTS Magnet System (MS), which have the shape of bulk cylindrical discs. These samples are encased in an aluminium container and then coated in styrofoam for protection [35,36].

Many studies have been published for measuring the flow rate of conducting liquid using large electromagnets and sensing devices with an electronic system leading to an expensive and colossal size for installation of flow sensors. To overcome these limitations, a flow sensing system comprising a pair of electrodes with a signal condition circuit is recommended, which involves lesser cost and enables the small size.

#### 4. Applications of Electric Field as Source of Excitation: Theory And Working Principle

This section enumerates the concepts of electrostatic induction, cross-correlation, and polarisation impedance methods using several theoretical approaches for measuring the flow rate with an electric field based source of excitation. Researchers have described the various technologies for measuring low conductive fluid flow using fundamental concepts validated by experimental and numerical simulations.

There are distinct kinds of non-invasive methods for measuring the velocity of conductive fluids based on the electrostatic induction phenomenon. Mustafa [37] proposed a non-intrusive electrostatic system in 2011 for determining the velocity of charged fluid particles in a plastic Acrylonitrile-Butadiene-Styrene (ABS) pipe. The plastic pipe comprises ring-shaped sensing electrodes arranged in a particular fashion and placed adjacent to the conductive fluid flow. The complete assembly is protected circularly with an electromagnetic screen to avoid external perturbations, as shown in Figure 16(a).

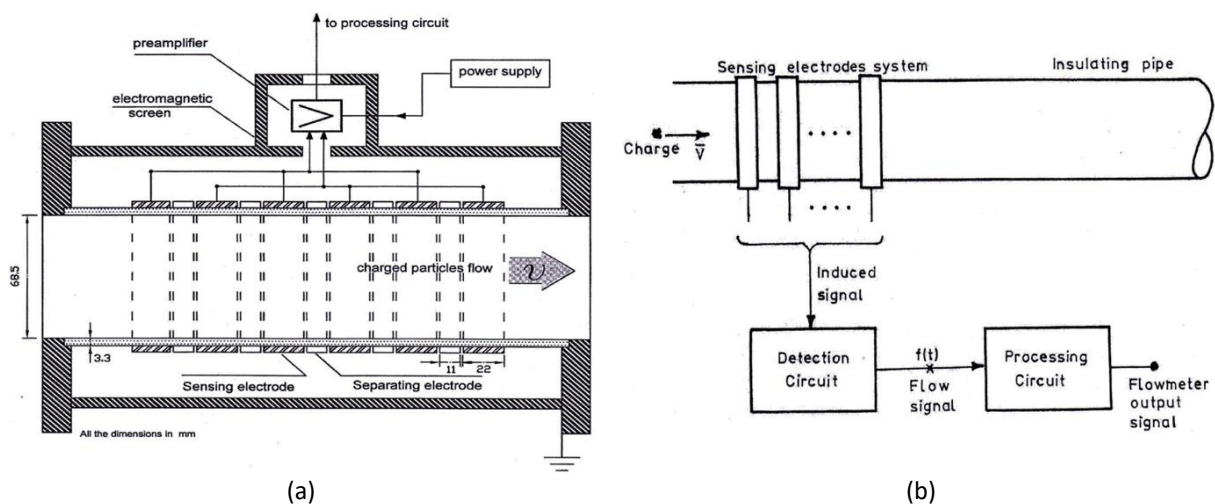


**Fig. 16.** Schematic view of electrostatic non-invasive method [37]; (a) Electrostatic induction, (b) Signal conditioning circuit

The movement of electrostatic charges carried by the fluid flow over the region of electrodes generates the electric potential between the sensing electrodes by using electrostatic induction defined in Eq. (8).

$$w = vK . \tag{8}$$



where  $w$  is mean frequency,  $K$  is constant for the particular geometry of the flowmeter, constant flow velocity, and its velocity profile. The detected flow signal from the sensing electrodes is processed by the processing circuit, which consists of a differentiator, an absolute value circuit, and a simple low-pass filter, as shown in Figure 16(b). The processing circuit is calibrated with a different set of sinusoidal frequencies. The frequency bandwidth range must be increased to detect the flow patterns in a wide range. Gajewski [38,39] discussed the flow of charged particles through the inductive ring probe rectilinear along its geometric axis without interruption. Figure 17(a) illustrates a thin strip of circle ring probe firmly attached to a portion of opaque dielectric duct section that isolates it from the fluid flow. The inner and outer diameters of the pneumatic pipeline, which is often made of metal, are identical to those of the dielectric pipeline.

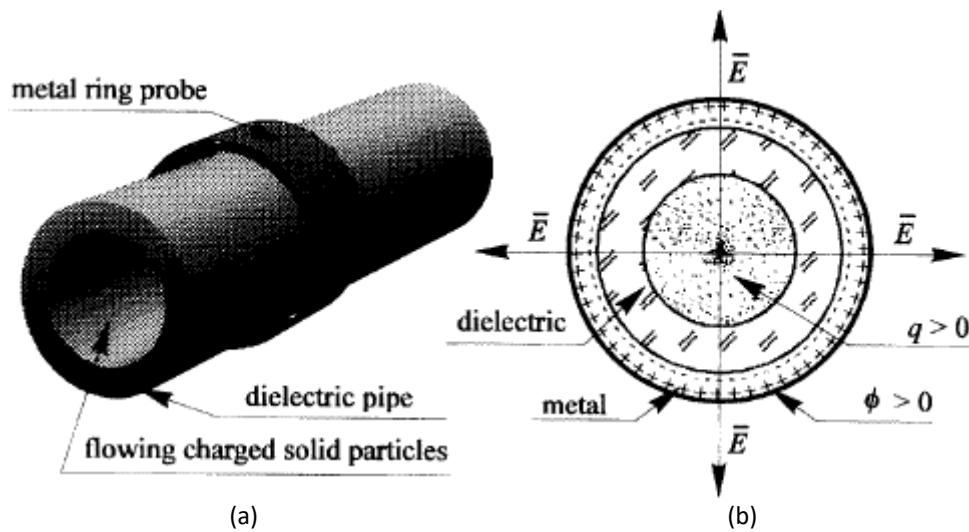


**Fig. 17.** Schematic View of the Electrostatic Inductive Ring [38]; (a) Metal ring on dielectric pipe, (b) Distribution of electric charges inside the duct

Figure 17(a) shows that the dielectric pipe allows the electric field  $E$  to the inductive probe ring, produced by the passage of fragments of charged solid particles inside the sensitive zone. The electric potential  $\phi$  and charge  $q$  are induced on an inductive ring as shown in Figure 17(b). The width of an inductive probe should be as small as possible so that the input signal can be separated more accurately and the bandwidth can be increased.

Beck [40] have discussed the cross-correlation method based on fluid flow movement in a duct. The fluid flow travels from upstream signal  $x(t)$  to downstream signal  $y(t)$ , as shown in Figure 18. The cross-correlation of the two signals is defined in Eq. (9).

$$R_{xy}(\tau) = \lim_{T \rightarrow \infty} \frac{1}{T} \int_0^T y(t)x(t - \tau)dt \quad (9)$$

where  $R_{xy}(\tau)$  is the cross-correlation function.

Through the time location of the most significant cross-correlation coefficient, it is possible to calculate the time delay,  $\tau$  between the two signals. The cross-correlation coefficient is computed using Eq. (10).

$$\rho_{xy}(\tau) = \frac{R_{xy}(\tau)}{\sqrt{R_{xx}(0)R_{yy}(0)}} \quad (10)$$

where  $R_{xy}(\tau)$  is the cross-correlation function of  $x$  and  $y$  at time delay  $\tau$ .

$R_{xx}(0)$  and  $R_{yy}(0)$  are the cross-correlation functions of  $x$  and  $y$  at the time position of zero.

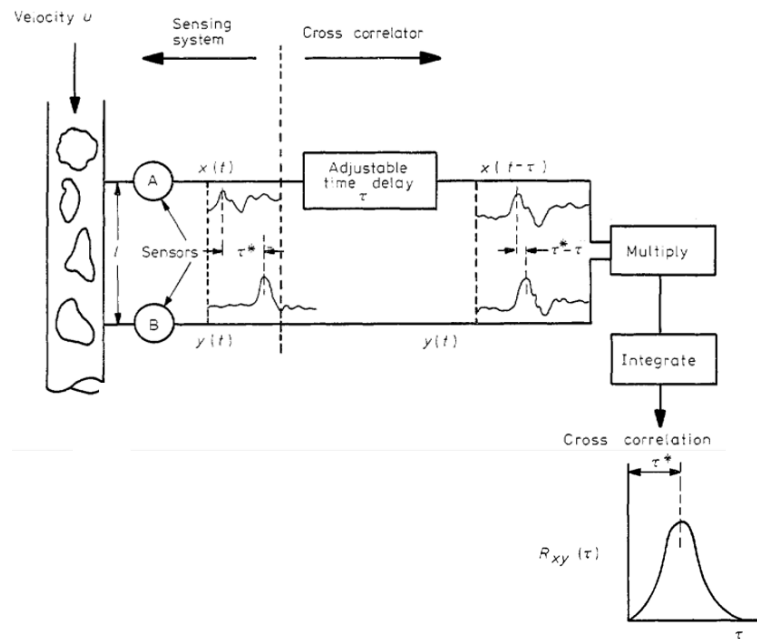


**Fig. 18.** Cross-Correlation principle for flow measurement [40]

The flow rate of conductive fluids was measured through conductive signals of the fluid flow [41,42]. Based on studies by Huang *et al.*, [43] and Zemann *et al.*, [44] independently presented the new method known as Capacitively Coupled Contactless Conductivity Detection (C<sup>4</sup>D) for the measurement of conductivity. The electrodes of a C<sup>4</sup>D sensor do not come in contact with the fluid being measured. In addition to the study, Ji *et al.*, [45] proposed a novel non-invasive method for the measurement of flow rate in millimetre-scale pipes using the combination of the C<sup>4</sup>D technique and the principle of cross-correlation. Two steps are involved in measuring the flow rate of conductive fluids; in the first step, two conductivity signals were obtained by the novel five-electrode C<sup>4</sup>D sensor. In the second step, the cross-correlation concept was applied to the obtained signals.

Five C<sup>4</sup>D sensor consists of an excitation, one metal electrode subjected to an AC voltage. Three pick-up metal electrodes collected the output signal and it was fed to the data acquisition unit. Finally, the fourth electrode is grounded. Electrodes are arranged cylindrically around the exterior of the insulating pipe as shown in Figure 19(a). The coupling capacitances formed by the insulating pipe, five metal electrodes, and the conductive fluid are denoted as  $C_{x1} \sim C_{x4}$ . The fluid between the two neighbouring electrodes is denoted as  $R_{x1} \sim R_{x4}$ . An alternating closed path is formed by  $C_{x1}, C_{x5}$  as shown in Figure 19(b). When an alternating voltage  $V_{in}$  is supplied to the excitation electrode, an alternating current flows across the AC route. The resulting alternating current is defined in Eq. (11).

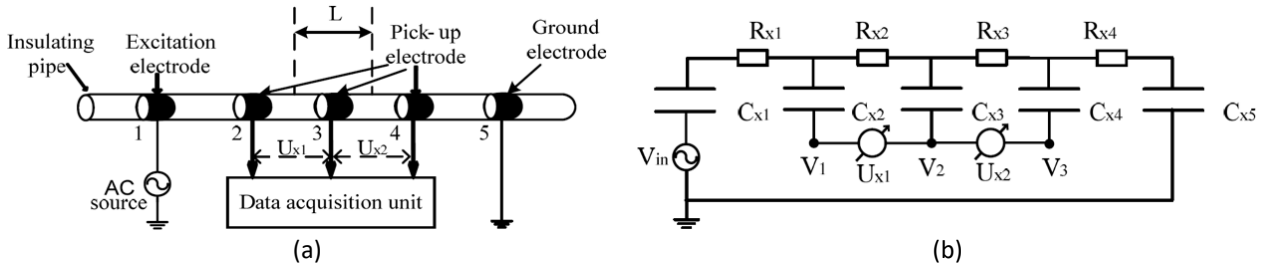


**Fig. 19.** Schematic View of  $C^4D$  sensor with the principle of cross correlation [45]; (a) Five  $C^4D$  sensor [45], (b) Equivalent circuit [45]

$$I = \frac{V_{in}}{R_{x1} + R_{x2} + R_{x3} + R_{x4} - j \left[ \frac{1}{2\pi f C_{x1}} + \frac{1}{2\pi f C_{x5}} \right]} \quad (11)$$

The differential voltages  $U_{x1}$  and  $U_{x2}$  shown in Figure 19 represent the two conductivity signals information between electrodes 2 and 3 (upstream sensor) and electrodes 3 and 4 (downstream sensor). Cross-correlation of the two conductivity signals (i.e.,  $U_{x1}$  and  $U_{x2}$ ) determines the time delay  $\tau$  shown in Figure 20(a), which is obtained by the time position of the largest cross-correlation coefficient as shown in Figure 20(b).

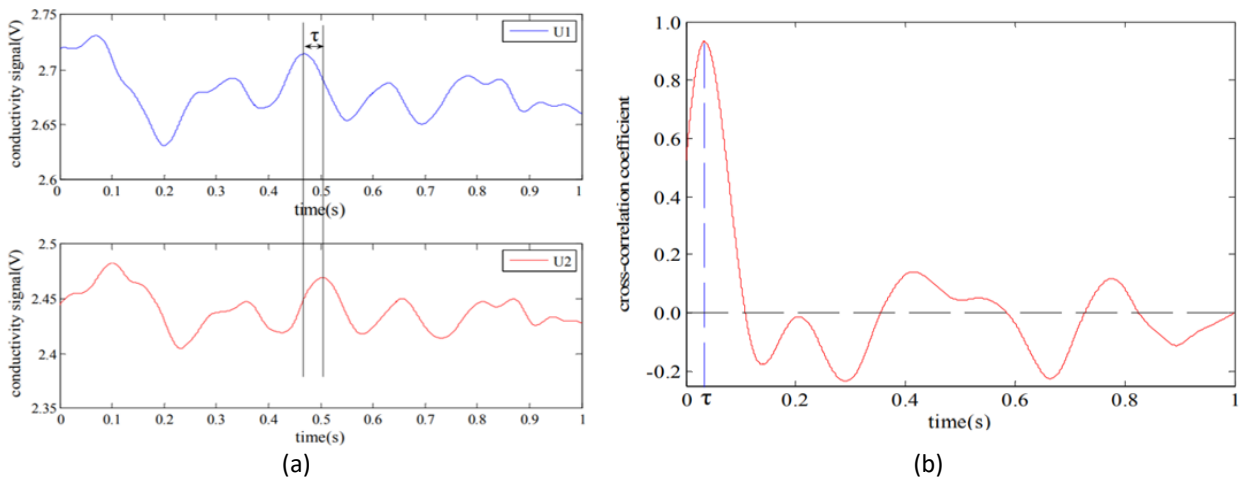


**Fig. 20.** Measurement of fluid flow [45]; (a) Conductivity signals, (b) Cross-correlation coefficient of conductive signals

The average fluid velocity is given by Eq. (12).

$$V = \frac{L}{\tau} \quad (12)$$

where  $L$  is the separation distance between the centre of a combination of electrodes (i.e., 2 and 3 ; 3 and 4). The experimental findings demonstrated the viability of the suggested approach for measuring flow rate satisfactorily. The most considerable relative discrepancy between the observed flow rate and the reference flow rate in five millimetre-scale pipes with varying inner diameters of 0.8, 0.5, 1.8, 3.0, and 3.9 mm is less than 5%.

Electromagnetic Capacitance Tomography (ECT) measured the electrical capacitance between the parallel plates on the pipe's edge to determine the flow rate, density, concentration, impurity level, and permittivity of a fluid or fluid mixture [46]. Electrodes that serve as both sources and detectors surround the item being scanned in tomography. The electrodes are activated one at a

time or in pairs depending on the technique. At any given instant, just one or a pair of electrodes is activated. In contrast, the remaining electrodes serve as a detector, since the capacitance of any two electrodes may be monitored using the sequence of activating a pair of electrodes. As a result, various methods can be developed. The sensor is made up of a series of electrodes that are positioned around the perimeter of the pipe. The electrode length may be reduced because of the higher cover angle of electrodes, resulting in enhanced inter-electrode capacitance. It is worth noting that capacitance is related to electrode size for a given diameter of sensor. The fringe effect and the lowest capacitance are the two main factors that restrict the length of electrodes. If the length of electrodes is sufficiently long, then the fringe effect is neglected. Internal and external electrode installations are the two different kinds. The electrode is typically installed externally since it is easier to install, design, and fabricate.

External electrodes are commonly mounted outside of an insulating frame. Furthermore, external electrodes are non-intrusive and are not exposed to high temperatures or turbulent conditions. However, because the wall capacitance is essentially in series with the internal capacitance, it negatively influences the measurement of the internal capacitance, as discussed in Yang [47]. It would be challenging to separate the internal capacitance from the measured capacitance if the reactance of the wall is excessively high (i.e., the wall capacitance is too small because of the thicker wall). In this regard, the thinner wall improves the performance of sensor. Pressure often controls wall thickness in real-world situations. The thickness of sensor walls typically range from 2 to 4 mm. Sandwiching measuring electrodes between two insulating layers would allow for using a thin wall with high pressure. Sandwiching measuring electrodes between two insulating layers would suit thin walls under high-pressure conditions.

The driven guards are connected at the end of the measurement electrodes as shown in Figure 21. The arrangement of electrodes indicates the prevention of electric field from propagating in the axial direction. This configuration might alleviate the fringe effect, allowing a much better signal to be detected from a measurement electrode.

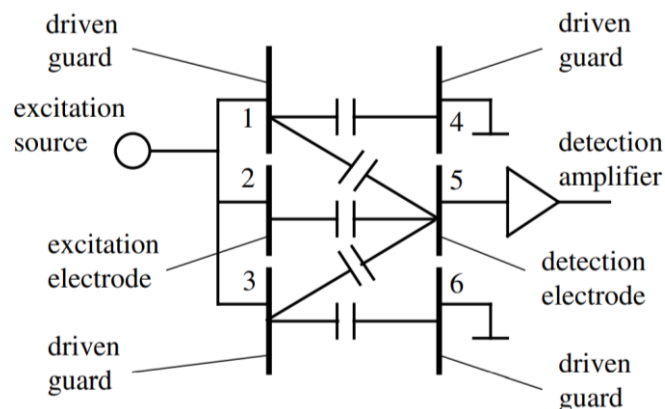


**Fig. 21.** Electrical capacitance tomography [47]

Abegaz *et al.*, [48] discussed the non-invasive measurement of the water flow in a conduit using the concept of Electrical Capacitance Tomography (ECT). The ECT technique relies on measuring capacitances from multiple electrodes along the surface of the fluid-carrying pipe. The data could be used to monitor and quantify the flow of water in pipes or ducts, which is a new aspect of the method. The flow velocity of water in a pipe was measured to be 0.2936 m/s, while the volumetric flow rate was  $5.96 \times 10^{-4}$  m<sup>3</sup>/s using the proposed method. Capacitance tomography was accomplished by utilizing parallel plate capacitors with 2, 4, and 6 electrodes. The speed of fluid flow was found by dividing the distance between two capacitive plates on the pipe's surface by the time it took for the

fluid to move through the pipe. An inductor surrounding the pipe and monitoring the change in inductance dependent on the flow might be used to measure fluid flow. However, capacitance-based fluid flow monitoring is preferable since it detects ferromagnetic materials and other solid, liquid, or gaseous materials with varying degrees of sensitivity.

The suggested measuring approach relies on a traceless flow metre that uses cross-correlation and has the potential of universal applicability to all varieties of fluid flow. This is so because it doesn't need to change physically. The force measurement depends on the noise pattern captured in an externally observable process variable, with the transit time as fluid moves from point A to point B, as shown in Figure 22.

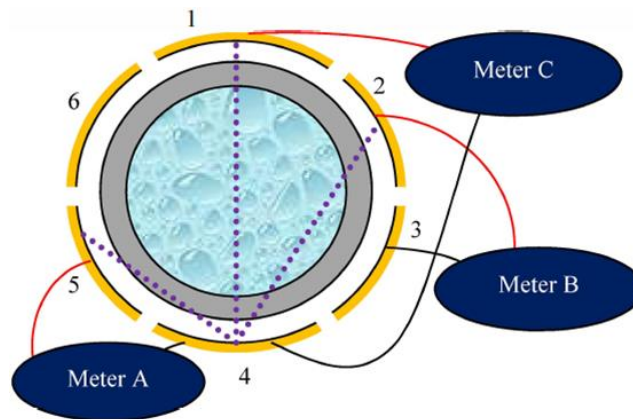


Fig. 22. Position of capacitors on surface of pipe [48]

Bera and Mandal [49] discussed the non-invasive capacitance type orifice transducer for measuring the volumetric flow rate of low-conductive liquid through the pipe channel. The diaphragm system of a DP cell senses the differential pressure generated across the orifice in an orifice-type transducer. The mechanical movement of the diaphragm system is transformed into a pneumatic or electrical signal by employing a flapper nozzle, strain gauge, or piezoresistance-type transducers. However, these DP cell-type orifice transducers are prone to inaccuracy due to fluid leakage, changes in the elastic property of material of diaphragm and the corrosive influence of process fluid. This transducer is a capacitance between a metal orifice plate 'DJ' and a close-by grounded metal ring 'HK'. The metal ring surrounds an insulating pipe connected to a grounded metal main pipe or between an insulated metal orifice and the conducting pipe.

A vena-contracta zone is concentrated at point 'C' on the downstream side of the orifice plate when fluid passes through an aperture in a pipeline. 'EF' is at a minimal distance "xo" from the orifice plate represents the cross-section of the conical fluid flow in the plane of 'HK,' as illustrated in Figure 23. This occurs close to the orifice plate. The length and diameter of vena-contracta region are proportional to its flow rate. Consequently, the flow rate affects the capacitance in the vena contracta area between an insulated orifice and an electrode that is exceptionally close to the orifice. If the pipeline is composed of conductive material and comes in contact with the conducting liquid, it can serve as the second electrode of sensing capacitor. The capacitance between the orifice plate DJ and ring HK is believed to be equal to the capacitance ( $C_x$ ) between the orifice plate and the liquid jet section EF.

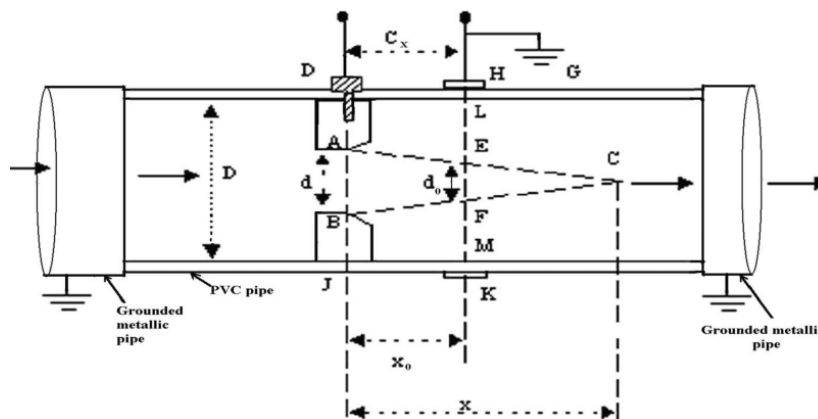


Fig. 23. Schematic view of capacitance orifice transducer [49]

Consequently, the Eq. (13) can represent this capacitance:

$$C_x = \frac{\epsilon_0 k A'_0}{x_0} \tag{13}$$

where  $\epsilon_0$  is the permittivity of the vacuum and  $A'_0$  is effective overlap area between section EF of the fluid flow jet and the orifice plate DJ,  $k$  is dielectric constant and  $x_0$  is the distance between the orifice plate and the metal ring enclosed by the duct.

Positive and negative ions created by dissociating molecules in the dielectric liquid produce the electric current. Because there is no charge injection at the electrodes, electric charges produced by dissociation are attracted to the opposite polarity electrode [50]. They accumulate in the region of that electrode and form a hetero charge layer as shown in Figure 24(a). The accumulated layer has opposite polarity to the adjacent electrode. It generates a space charge near the electrodes by injecting electrons into the liquid and binding to neutral molecules to generate ions. The build-up of electric charges causes the formation of a non-neutral layer made up of ions with the same polarity as the electrode, known as the homocharge layer, as shown in Figure 24(b). The electrode then repels electric charges. An electric "double-layer" exists (i.e., across either a heterocharge layer or a homocharge layer) when a metal electrode is in contact with a conductive liquid at the metal-liquid interface [51,52].

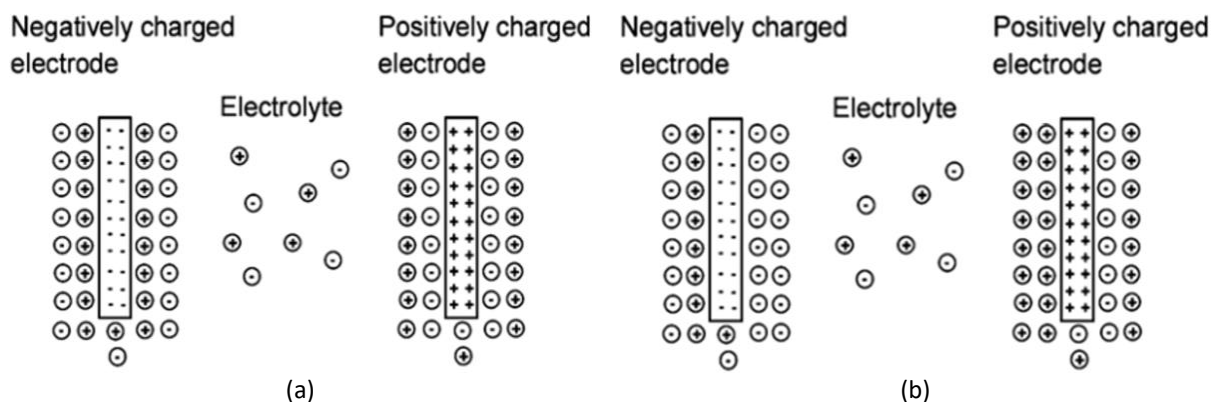


Fig. 24. Formation of layers between the electrodes and dielectric liquid [50]; (a) Heterocharge layer, (b) Homocharge layer

One charge layer is placed at the metal interface. An equal and opposite electrical charge resides on the other layer. Hence, the liquid possesses opposite polarity [53,54]. The "double layer" of charge resembles a parallel plate capacitor in its behaviour, and the interface capacitance is known as double-layer capacitance or polarisation capacitance  $C_p$ . The process of ion diffusion to and from the metal interface over the double layer encounters 'charge transfer' resistance or polarisation resistance,  $R_p$ . The electrode polarisation impedance,  $Z_p$  is written in terms of capacitance and resistance values using Eq. (14).

$$Z_p = R_p + \frac{1}{j\omega C_p} \quad (14)$$

Once a further electrode is connected throughout the system, the DC boundary potential occurs between electrodes and electrolyte. When a small sinusoidal voltage signal is supplied across the electrodes, the AC voltage signal is overlaid with the (DC voltage) half-cell potential at each electrode, resulting in the flow of ions from one electrode to the other [55]. Ohmic and polarisation impedance of the liquid between the electrodes may oppose the electric current caused by the flow of ions. If there is a liquid flow from one electrode to the other, the viscous effect of the liquid caused by the velocity gradient resists the flow of ions. As a result, the net impedance between the electrodes, which is defined as the ratio of "supply voltage to current", relies on the effects of electrode polarisation, Ohmic, and the velocity gradient of fluid flow [55].

In 2009, Bera and Chakraborty [56] conceptualized and designed a flow metre to monitor conductive liquid flow rate based on the theory of electrode polarisation. It is one of the most basic, low-cost flow metres for calculating the flow rate of conductive fluid. This method uses four indistinguishable metallic stainless steel electrodes, each measuring 15mm in length, and injected into the one-inch diameter of the pipeline section at a depth of 2mm with adequate insulation, as shown in Figure 25.

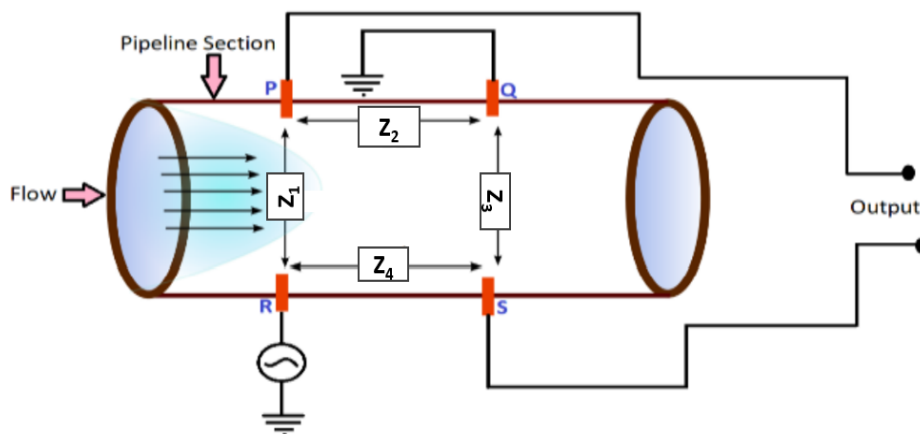
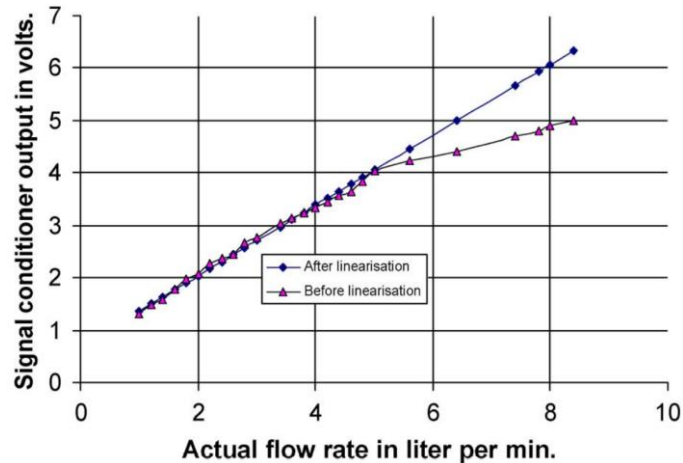


Fig. 25. Polarisation impedance-based fluid flow measurement system [56]

The positioning of the electrodes in the pipeline portion is utilized to develop the flow metre. The electrodes are implanted so that the two electrodes are placed in series with a 3cm set space between them. Two additional electrodes are positioned diametrically opposite these two electrodes. The electrodes are installed in the pipeline segment to cause the slightest hindrance in the flow path. As shown in Figure 25, any two crosswise-positioned electrodes are utilized to provide input signal, while the other two are employed to receive the output signal. The authors have assumed that the four electrodes are equivalent to four lumped impedances and form a Wheatstone bridge network. Two cross electrodes are subjected to a small sinusoidal voltage of 5V at 1000Hz. In

this research, the Bera *et al.*, assumed that the liquid flow rate depends on the polarisation impedance of electrode, holding all other parameters constant. A change in the flow rate causes variation in the polarisation impedance throughout the pipeline section. It is assumed that the polarisation impedance over a cross section along the axis of the channel is constant since there is no velocity component of the fluid across the diameter of the pipeline segment. The output signal of the polarisation impedance-based flowmeter is linearly dependent on the change in liquid flow rate in the laminar flow condition as shown in Figure 26.



**Fig. 26.** Conditioned output signals for the actual flow rate [56]

In a scenario of turbulent flow, the polarisation impedance-based flow metres exhibit non-linear output. The suggested bridge-circuit near-balanced state reduces the non-linear nature of the output. An experiment was conducted for the conductive fluid flow of 300–400 S/m and a flow rate of 1.025–8.4LPM. The suggested flow meter output has been conditioned to 1-5V using a signal-conditioning unit. When subjected to AC signal over a broad range of frequencies up to 25 kHz with a peak amplitude of 5 V, the sensitivity of sensor's output to flow rate ranging from 1 LPM (60 LPH) to 10 LPM (600 LPH) is very weak. This is due to the superimposition of DC bias on the pure AC sinusoidal signal.

Yan and Sabic [57] developed a flow sensor in 2013 based on the polarisation impedance of electrode that can monitor the low flow rate of conductive liquid between 1.06 LPH and 25.18 LPH in a 20 mm diameter pipeline. The flow sensor is a conventional four-electrode system with two current-carrying electrodes and two output pick-up electrodes. Two current-carrying electrodes were subjected to a sinusoidal peak voltage of 2 V at 1000 Hz. It comprises two pairs of stainless steel electrodes separated by a distance of 16mm. Each pair of electrodes is positioned symmetrically on opposite sides of the duct and is placed into a non-conductive flow tube, as shown in Figure 27. The polarisation impedance of the two current-carrying electrodes is influenced by flow rate, resulting in a differential potential observed between the two pick-up electrodes. The flow sensor segment is attached to the pipeline with flanges that have the same internal diameter as the pipeline to prevent disturbance in flow.



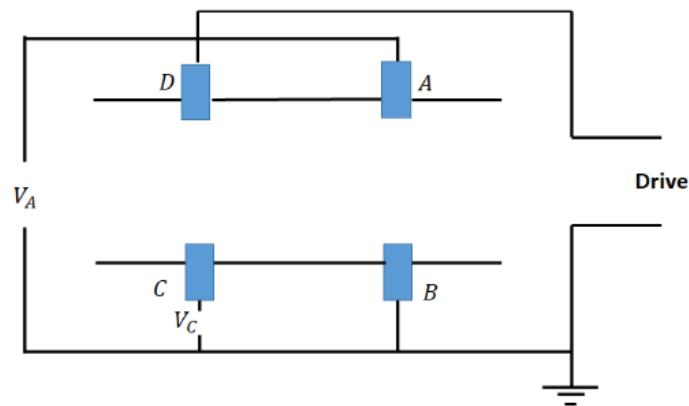


Fig. 27. Excitation of electrodes placed into duct [57,58]

The depletion and regeneration of ions close to the interface of metal and electrolyte cause the flow velocity to impact the polarisation impedance of electrode. An increased flow rate decreases the conductance of the solution, which raises the resistive component of polarisation impedance of electrode. The differential voltage among the two electrodes decreases as the resistive portion of polarisation impedance of electrode increases.

The flow sensor's output voltage varies non-linearly as the flow rate changes. The non-linear nature of the sensor's output indicates that the proposed flow sensor is insensitive to measuring high flow rates. The responses of the electrode polarisation impedance-based flow sensor are shown in Figure 28 when it is excited with a sinusoidal voltage of 2 V at a frequency of 1000 Hz and with a DC offset value of +8, +4, 0 and -4 V, respectively. The findings revealed an average of 50 observations of the differential peak-to-peak potential amplitude was obtained every 20 cycles for each flow rate.

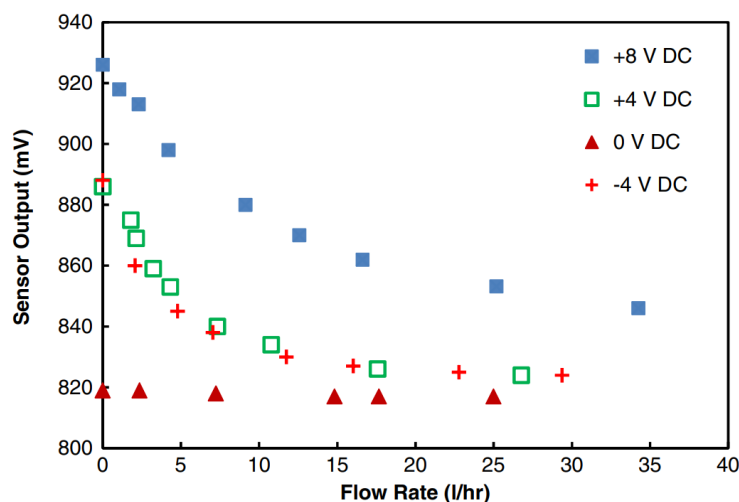


Fig. 28. Variation in Sensor output with flow rate change in DC offset voltage [57,58]

Yu *et al.*, [59] suggested a novel PolyDiMethylSiloxane (PDMS) flow sensor to measure the amount of conductive liquid. The flow sensor is made up of two sets of metal electrodes that are made in the PDMS channel. The conductive liquid flow is uniformly accelerated in the homogenous microfluidic channel under stable pressure difference. When the liquid flows through the flow sensor, the volume of liquid is measured using the time-of-flight of the resistance of the pair of electrodes. The displayed flow sensor performs admirably for conductive liquid. The uniformly accelerated conductive liquid passes the section of electrodes during the time interval, which results in the

computed conductive liquid volume. The received signal is collected in a computer through a data acquisition interface.

Maurya *et al.*, [60] described an optical communication method based on Mach–Zehnder Interferometer (MZI). Signal transmission over an optical communication system is becoming more popular since the transmitted signal is free of measurement errors caused by electromagnetic interference. The suggested technique includes only four insulated conducting electrodes in contact with the fluid flow. In a signal conditioning circuit, an electro-optic system is used, and it transmits the measured signal to remote places. A lumped polarisation impedance between the electrodes act as the bridge arms and forms the bridge network which is used to examine the performance of the sensor and transmission system. Theoretical equations have been derived to explain the working of a bridge network using a stable sinusoidal AC source and an electro-optic system based on MZI. The electro-optic unit employs the MZI principle to transform the electrical output into an optical signal that can be easily transferred across the fibre-optic medium. Therefore, the suggested transmitter unit will have a little time lag and less power consumption. The electric field-generating device will require a nominal current from the source (i.e. the signal conditioner). Consequently, the loading effect error of measuring unit will be small. The developed measurement system has excellent repeatability and linearity. It is suitable for usage in the flammable region.

Ayliffe and Rabbitt [61] suggested a microelectromechanical flow sensor for measuring the flow rate of ionic solution. The micro-flow sensor uses glass wafers and features a fluid channel with a cross-section size of  $4 \times 10 \mu\text{m}^2$ . The micro-flow sensor is made up of two gold microelectrodes that are attached to the sidewalls of the channel. The flow rate of the ionic solution with 0.9% concentration between the pairs of gold electrodes is 2.4 and 4.8  $\mu\text{LPM}$ . Maximum sensitivity of the flow sensor was found at 350Hz with an appropriate DC offset voltage of 50 mV. The origin of the electric impedance was investigated using an electrochemical convection-diffusion model. According to the model, transmitting a direct current among the gold electrodes increased the ionic concentration in the micro-domain between the electrodes. This variation results from the counterbalancing ions necessary to maintain the neutrality of space-charge moving towards the electrode surfaces. The higher ionic concentration washes away from electrodes. It is replaced with the bulk solution as the rate of fluid flow increases, resulting in a decrease in the average ionic concentration inside the recording zone. The decrease in net concentration of available ions between the electrodes results in change in polarization resistance. This method is straightforward, widely acceptable, and economical method for estimating the flow rate of an ionic solution. The degree of polarisation impedance depends on various parameters, including the distance between the electrodes, current density, frequency, electrode material, electrode area, electrode shape, temperature, and ions concentration.

From the review of findings of the past research, the range of electrical conductivity of fluid and flow velocity for various non-invasive measurement techniques are listed in Table 2.

It has been proved that each non-invasive measurement technique has its limitations based on the source of excitation (either magnetic or electric fields). Different values of low conductivity of fluid and flow velocity have been considered in various studies to analyse the capability of the identified techniques so that their scope and versatility can be researched further.

Apart from all these investigations, the thermal conductivity of fluid and velocity slip conditions also impact the flow rate measurement. The profile of fluid velocity gets disturbed due to the alignment and inclination of either the magnetic field or electric field. Consequently, the thickness of boundary layer increases [62-68].

**Table 2**  
 Various non-invasive measurement techniques

Author	Technique	Non-Invasive		Range of Electrical conductivity (S/m)	Range of Flow velocity (m/s)
		Intrusive	Non-Intrusive		
Sakurai and Ishihara [18]	Capacitance Type electromagnetic flow meter	Yes	No	$1 \times 10^{-5} \leq \sigma \leq 2 \times 10^{-3}$	$0.5 \leq v \leq 10$
Wegfrass <i>et al.</i> , [25]	Principle of deflection based on Lorentz Force	No	Yes	$2.3 \leq \sigma \leq 14.0$	$0.8 \leq v \leq 4.0$
Vasilyan and Froehlich [27]	Lorentz Force based on EMC	No	Yes	$2 \leq \sigma \leq 20$	$v \leq 2.5$
Fröhlich <i>et al.</i> , [33]	Lorentz Force based on EMC	No	Yes	$\sigma < 6$	$0.2 \leq v \leq 3$
Resagk and Ebert [34]	Lorentz force based on Buoyancy based Weight Force Compensation	No	Yes	$1 \leq \sigma \leq 10$	$0 \leq v \leq 3.5$
Mustafa [37]	Electrostatic method	No	Yes	Insulating Liquids	$2 \leq v \leq 50$
Ji <i>et al.</i> , [45]	C <sup>4</sup> D and Cross-correlation	No	Yes	$0.01865 \leq \sigma \leq 1.321$	$0.6 \leq v \leq 2.32$
Abegaz <i>et al.</i> , [48]	electrical capacitance tomography	No	Yes	$0.07 \leq \sigma \leq 0.3$	Till 0.2936
Bera and Mandal [49]	capacitance-type orifice transducer	Yes	No	Conductive Fluid (Range not mentioned)	$0.05 \leq v \leq 0.3$
Bera and Chakraborty [56]	Polarisation impedance realization by bridge-type technique	Yes	No	$3 \times 10^{-4} \leq \sigma \leq 4 \times 10^{-4}$	$0.05 \leq v \leq 0.44$
Yan and Sabic [57]	polarization impedance	Yes	No	$5 \times 10^{-4} \leq \sigma \leq 8 \times 10^{-4}$	$0.009 \leq v \leq 0.022$
Maurya <i>et al.</i> , [60]	MZI-based electro-optic system	Yes	No	$5 \times 10^{-4} \leq \sigma \leq 6 \times 10^{-4}$	$0.005 \leq v \leq 0.53$

#### 4. Concluding Remarks

This paper provides an overview of principles, methodology and applications for the non-invasive measurement of a flow rate of low conductive fluid. The measured average velocity through the channel depends on various parameters such as electrical conductivity, Lorentz force, polarisation impedance, transfer of charge particles by induction, and capacitance formation between metal electrodes. Many observations have resulted from the review presented in this paper, and the same can be summarised as follows

- i. An electric polarisation impedance exists when metallic electrodes are in contact with the conductive fluid flow. The net polarisation impedance relies on the capacitance between the electrodes, Ohmic impedance and gradient in the velocity.
- ii. The arrangement of excitation electrodes and pick-up electrodes across the measuring pipeline section decides the behavioural characteristics of the flow sensor.
- iii. Emerging technologies like cryostats with superconducting magnet systems, which unquestionably exceed the mass limitation, have become viable applications for Lorentz force velocimetry.

- iv. Resolution of Lorentz force can be improved by implementing the electromagnetic force compensation scheme and buoyancy based Weight Force Compensation (WFC).
- v. The magnetic systems are improvised by involving the Halbach array and high temperature super conducting magnets.
- vi. The passage of electric charges in fluid flow within the channel (duct) induces the electric potential among the metal electrodes. The mean frequency obtained by the electrode signals varies with the velocity of the flow at constant flow geometry and velocity profile.
- vii. The cross-correlation of conductive signals of the conductive fluid flow can also determine the flow velocity

From the emerging technologies to the relevance of the sources of excitation, it is highlighted that the flow rate of conductive fluid depends on pipe geometry comprising the parameters of size, diameter, velocity profile and thickness of material of duct. The response from the signal conditioning circuit varies either linearly or non-linearly with the flow rate. The turbulent flow shows the non-linear response, and the DC offset voltage improves the resolution. Development of the various sensor configurations for measuring the flow velocity of conductive fluid within the duct over a varying range of velocity will be of practical significance. Similarly the characterization of the performance of sensing element in a flow meter when subjected to varying material properties of the duct wall will be also of interest from the perspectives both research and practical applications. Similarly, the detectable magnetic field and electric field on the surface of the metallic duct and its effects on the velocity profile of fluid flow are also of interest for future research.

### Acknowledgement

This research was not funded by any grant.

### References

- [1] Sproston, John L. "Flow measurement future directions." *Sensor Review* 22, no. 3 (2002). <https://doi.org/10.1108/sr.2002.08722caa.002>
- [2] Pereira, Miguel. "Tutorial 20: flow meters: part 2-Part 20 in a series of tutorials in instrumentation and measurement." *IEEE Instrumentation & Measurement Magazine* 12, no. 3 (2009): 21-27. <https://doi.org/10.1109/MIM.2009.5054549>
- [3] Smith, Jonathan. "Flowmeter review." *Sensor Review* 15, no. 4 (1995): 11-14. <https://doi.org/10.1108/02602289510102318>
- [4] Pereira, Miguel. "Flow meters: part 1." *IEEE Instrumentation & Measurement Magazine* 12, no. 1 (2009): 18-26. <https://doi.org/10.1109/MIM.2009.4762948>
- [5] Shercliff, John Arthur. *The theory of electromagnetic flow-measurement*. CUP Archive, 1962.
- [6] Lincoln, David. *Investigation into an electromagnetic flowmeter for use with low conductivity liquids*. Cardiff University (United Kingdom), 2006.
- [7] Doebelin, Ernest O., and Dhanesh N. Manik. *Measurement systems: application and design*. McGraw-Hill, 2007.
- [8] Bentley, John P. *Principles of measurement systems*. Pearson Education, 2005.
- [9] Baker, Roger C. *Flow measurement handbook: industrial designs, operating principles, performance, and applications*. Cambridge University Press, 2016. <https://doi.org/10.1017/CBO9781107054141>
- [10] Lipták, Béla G. *Process measurement and analysis*. CRC Press, 2003.
- [11] LaNasa, Paul J., and E. Loy Upp. *Fluid flow measurement: A practical guide to accurate flow measurement*. Butterworth-Heinemann, 2014. <https://doi.org/10.1016/B978-0-12-409524-3.00003-4>
- [12] Pirow, Nicol Oswald. "Development of a non-invasive water flow meter for a smart geyser." *PhD diss., Stellenbosch Stellenbosch University*, 2018.
- [13] Levenspiel, Octave. "Flow of Incompressible Newtonian Fluids in Pipes." In *Engineering Flow and Heat Exchange*, pp. 19-41. Springer, Boston, MA, 1998. [https://doi.org/10.1007/978-1-4899-0104-0\\_2](https://doi.org/10.1007/978-1-4899-0104-0_2)
- [14] Nour, Maha A., and Muhammad M. Hussain. "A review of the real-time monitoring of fluid-properties in tubular architectures for industrial applications." *Sensors* 20, no. 14 (2020): 3907. <https://doi.org/10.3390/s20143907>

- [15] Walmsley, H. L., and G. Woodford. "The generation of electric currents by the laminar flow of dielectric liquids." *Journal of Physics D: Applied Physics* 14, no. 10 (1981): 1761. <https://doi.org/10.1088/0022-3727/14/10/011>
- [16] Stefani, F., and G. Gerbeth. "Velocity reconstruction in conducting fluids from magnetic field and electric potential measurements." *Inverse Problems* 15, no. 3 (1999): 771-786. <https://doi.org/10.1088/0266-5611/15/3/309>
- [17] Hussain, Y. A., and R. C. Baker. "Optimised noncontact electromagnetic flowmeter." *Journal of Physics E: Scientific Instruments* 18, no. 3 (1985): 210. <https://doi.org/10.1088/0022-3735/18/3/010>
- [18] Sakurai, Yutak, and Tami Ishihara. "Capacitance type electromagnetic flowmeter." *Flow Measurement and Instrumentation* 3, no. 7 (1996): 300. [https://doi.org/10.1016/S0955-5986\(97\)88079-X](https://doi.org/10.1016/S0955-5986(97)88079-X)
- [19] Polo, Jose, Ramon Pallàs-Areny, and J. P. Mardn-Vide. "Analog signal processing in an AC electromagnetic flowmeter." *IEEE Transactions on Instrumentation and Measurement* 51, no. 4 (2002): 793-797. <https://doi.org/10.1109/TIM.2002.803401>
- [20] Liu, Tiejun, Tongsheng Gong, and Yinjia Chen. "Development of an Electromagnetic Flowmeter with Dual Frequency Excitation." *TELKOMNIKA Indonesian Journal of Electrical Engineering* 10, no. 8 (2012): 2013-2019. <https://doi.org/10.11591/telkomnika.v10i8.1633>
- [21] Yang, Hong-Yu, Yan Chen, and Hui Zhao. "Signal acquisition and processing method for capacitive electromagnetic flowmeter." *Journal of Electronic Science and Technology* 19, no. 1 (2021): 100026. <https://doi.org/10.1016/j.jnlest.2020.100026>
- [22] Li, Bin, Yue Yan, Jie Chen, and Xinghang Fan. "Study of the ability of an electromagnetic flowmeter based on step excitation to overcome slurry noise." *IEEE Access* 8 (2020): 126540-126558. <https://doi.org/10.1109/ACCESS.2020.3008419>
- [23] Thess, Andre, Evgeny Votyakov, Bernard Knaepen, and Oleg Zikanov. "Theory of the Lorentz force flowmeter." *New Journal of Physics* 9, no. 8 (2007): 299. <https://doi.org/10.1088/1367-2630/9/8/299>
- [24] Wegfrass, André, Christian Diethold, Michael Werner, Thomas Fröhlich, Bernd Halbedel, Falko Hilbrunner, Christian Resagk, and André Thess. "A universal noncontact flowmeter for liquids." *Applied Physics Letters* 100, no. 19 (2012): 194103. <https://doi.org/10.1063/1.4714899>
- [25] Wegfrass, André, Christian Diethold, Michael Werner, Christian Resagk, Thomas Fröhlich, Bernd Halbedel, and André Thess. "Flow rate measurement of weakly conducting fluids using Lorentz force velocimetry." *Measurement Science and Technology* 23, no. 10 (2012): 105307. <https://doi.org/10.1088/0957-0233/23/10/105307>
- [26] Werner, M., B. Halbedel, and E. Rädlein. "Numerical study of magnet systems for Lorentz force velocimetry in electrically low conducting fluids." In *International Scientific Colloquium 'Modelling for Material Processing'(Riga, Latvia)*. 2010.
- [27] Vasilyan, S., and Th Froehlich. "Direct Lorentz force compensation flowmeter for electrolytes." *Applied Physics Letters* 105, no. 22 (2014): 223510. <https://doi.org/10.1063/1.4903235>
- [28] Halbedel, Bernd, Christian Resagk, André Wegfrass, Christian Diethold, Michael Werner, Falk Hilbrunner, and André Thess. "A novel contactless flow rate measurement device for weakly conducting fluids based on Lorentz force velocimetry." *Flow, Turbulence and Combustion* 92, no. 1 (2014): 361-369. <https://doi.org/10.1007/s10494-013-9505-5>
- [29] Vasilyan, Suren, Reschad Ebert, Markus Weidner, Michel Rivero, Bernd Halbedel, Christian Resagk, and Thomas Fröhlich. "Towards metering tap water by Lorentz force velocimetry." *Measurement Science and Technology* 26, no. 11 (2015): 115302. <https://doi.org/10.1088/0957-0233/26/11/115302>
- [30] Choi, Jae-Seok, and Jeonghoon Yoo. "Design of a Halbach magnet array based on optimization techniques." *IEEE Transactions on Magnetics* 44, no. 10 (2008): 2361-2366. <https://doi.org/10.1109/TMAG.2008.2001482>
- [31] Werner, Michael, and Bernd Halbedel. "Optimization of NdFeB magnet arrays for improvement of Lorentz force velocimetry." *IEEE Transactions on Magnetics* 48, no. 11 (2012): 2925-2928. <https://doi.org/10.1109/TMAG.2012.2196500>
- [32] Choi, Jae Seok, and Jeonghoon Yoo. "Optimal design method for magnetization directions of a permanent magnet array." *Journal of Magnetism and Magnetic Materials* 322, no. 15 (2010): 2145-2151. <https://doi.org/10.1016/j.jmmm.2010.01.047>
- [33] Fröhlich, Thomas, Michael Werner, Bernd Halbedel, and André Thess. "Lorentz Force Velocimetry for Poorly Conducting Fluids-Development and Validation of a Novel Flow Rate Measurement Device." In *International Conference on Electromagnetic Processing of Materials*. Beijing, China, 2012.
- [34] Resagk, C., and E. Ebert. "New developments on Lorentz force velocimetry for weakly conducting fluids." In *THMT-15. Proceedings of the Eighth International Symposium On Turbulence Heat and Mass Transfer*. Begel House Inc., 2015. <https://doi.org/10.1615/ICHMT.2015.THMT-15.1700>
- [35] Vakaliuk, Oleksii V., Mark D. Ainslie, and Bernd Halbedel. "Lorentz force velocimetry using a bulk HTS magnet system: proof-of-concept." *Superconductor Science and Technology* 31, no. 8 (2018): 084003. <https://doi.org/10.1088/1361-6668/aac949>

- [36] Vakaliuk, O., and B. Halbedel. "Lorentz Force Velocimetry using a bulk HTS magnet system." In *IOP Conference Series: Materials Science and Engineering*, vol. 424, no. 1, p. 012009. IOP Publishing, 2018. <https://doi.org/10.1088/1757-899X/424/1/012009>
- [37] Mustafa, Fawzi M. "Electrostatic nonintrusive method for measuring the flow rate of insulating fluids." *Journal of Basrah Researches (Sciences)* 37, no. 4A (2011): 15-24.
- [38] Gajewski, Juliusz B. "Electrostatic, inductive ring probe bandwidth." *Measurement Science and Technology* 7, no. 12 (1996): 1766. <https://doi.org/10.1088/0957-0233/7/12/012>
- [39] Gajewski, Juliusz B. "Electrostatic nonintrusive method for measuring the electric charge, mass flow rate, and velocity of particulates in the two-phase gas-solid pipe flows-its only or as many as 50 years of historical evolution." *IEEE Transactions on Industry Applications* 44, no. 5 (2008): 1418-1430. <https://doi.org/10.1109/TIA.2008.2002276>
- [40] Beck, M. S. "Correlation in instruments: cross correlation flowmeters." *Journal of Physics E: Scientific Instruments* 14, no. 1 (1981): 7. <https://doi.org/10.1088/0022-3735/14/1/001>
- [41] Fischer, Henry E. "An AC method of measuring the conductivity of dielectric liquids." *Master thesis, University of Missouri-Rolla*, 1966.
- [42] Sokolov, M., and M. Mashaal. "Velocity measurements in slow flow by the conductance-tracer method." *Experiments in Fluids* 9, no. 5 (1990): 252-256. <https://doi.org/10.1007/BF00233125>
- [43] Huang, Zhiyao, Jun Long, Wenbo Xu, Haifeng Ji, Baoliang Wang, and Haiqing Li. "Design of capacitively coupled contactless conductivity detection sensor." *Flow Measurement and Instrumentation* 27 (2012): 67-70. <https://doi.org/10.1016/j.flowmeasinst.2012.04.003>
- [44] Zemann, Andreas J., Erhard Schnell, Dietmar Volgger, and Günther K. Bonn. "Contactless conductivity detection for capillary electrophoresis." *Analytical Chemistry* 70, no. 3 (1998): 563-567. <https://doi.org/10.1021/ac9707592>
- [45] Ji, Haifeng, Xuemin Gao, Baoliang Wang, Zhiyao Huang, and Haiqing Li. "A new method for flow rate measurement in millimeter-scale pipes." *Sensors* 13, no. 2 (2013): 1563-1577. <https://doi.org/10.3390/s130201563>
- [46] Yang, W. Q. "Modelling of capacitance tomography sensors." *IEE Proceedings-Science, Measurement and Technology* 144, no. 5 (1997): 203-208. <https://doi.org/10.1049/ip-smt:19971425>
- [47] Yang, Wuqiang. "Design of electrical capacitance tomography sensors." *Measurement Science and Technology* 21, no. 4 (2010): 042001. <https://doi.org/10.1088/0957-0233/21/4/042001>
- [48] Abegaz, Brook W., Nathan T. Dick, and Satish M. Mahajan. "Measurement and characterization of fluid flow profile using electrical capacitance tomography." In *IEEE SOUTHEASTCON 2014*, pp. 1-8. IEEE, 2014. <https://doi.org/10.1109/SECON.2014.6950717>
- [49] Bera, Satish Chandra, and Haraprasad Mandal. "A flow measurement technique using a noncontact capacitance-type orifice transducer for a conducting liquid." *IEEE Transactions on Instrumentation and Measurement* 61, no. 9 (2012): 2553-2559. <https://doi.org/10.1109/TIM.2012.2192345>
- [50] Fricke, Hugo. "XXXIII. The theory of electrolytic polarization." *The London, Edinburgh, and Dublin Philosophical Magazine and Journal of Science* 14, no. 90 (1932): 310-318. <https://doi.org/10.1080/14786443209462064>
- [51] Daaboul, Michel, Philippe Traoré, Pedro Vázquez, and Christophe Louste. "Study of the transition from conduction to injection in an electrohydrodynamic flow in blade-plane geometry." *Journal of Electrostatics* 88 (2017): 71-75. <https://doi.org/10.1016/j.elstat.2017.01.014>
- [52] Vadde, Anusha, Govind R. Kadambi, and C. Siddabasappa. "An Electrohydrodynamic analysis for the characterisation of fluid flow within conducting and non-conducting channels." *Journal of Electrostatics* 119 (2022): 103746. <https://doi.org/10.1016/j.elstat.2022.103746>
- [53] Simpson, Raymond W., John G. Berberian, and Herman P. Schwan. "Nonlinear AC and DC polarization of platinum electrodes." *IEEE Transactions on Biomedical Engineering* 3 (1980): 166-171. <https://doi.org/10.1109/TBME.1980.326620>
- [54] McAdams, E. T., A. Lacknermeier, J. A. McLaughlin, D. Macken, and J. Jossinet. "The linear and non-linear electrical properties of the electrode-electrolyte interface." *Biosensors and Bioelectronics* 10, no. 1-2 (1995): 67-74. [https://doi.org/10.1016/0956-5663\(95\)96795-Z](https://doi.org/10.1016/0956-5663(95)96795-Z)
- [55] Onaral, B., and H. P. Schwan. "Linear and nonlinear properties of platinum electrode polarisation. Part 1: frequency dependence at very low frequencies." *Medical and Biological Engineering and Computing* 20, no. 3 (1982): 299-306. <https://doi.org/10.1007/BF02442796>
- [56] Bera, Satish Chandra, and Badal Chakraborty. "A novel technique of flow measurement for a conducting liquid." *IEEE Transactions on Instrumentation and Measurement* 58, no. 8 (2009): 2512-2517. <https://doi.org/10.1109/TIM.2009.2014620>
- [57] Yan, Tinghu, and Darko Sabic. "An electrode polarization impedance based flow sensor for low water flow measurement." *Measurement Science and Technology* 24, no. 6 (2013): 067002. <https://doi.org/10.1088/0957-0233/24/6/067002>

- [58] Lata, Anamika, and Nirupama Mandal. "Electrode polarization impedance and its application in flow rate measurement of conductive liquid: A review." *IEEE Sensors Journal* 21, no. 4 (2020): 4018-4029. <https://doi.org/10.1109/JSEN.2020.3029207>
- [59] Yu, Haixia, Dachao Li, Robert C. Roberts, Kexin Xu, and Norman C. Tien. "A micro PDMS flow sensor based on time-of-flight measurement for conductive liquid." *Microsystem Technologies* 19, no. 7 (2013): 989-994. <https://doi.org/10.1007/s00542-012-1686-7>
- [60] Maurya, P., S. K. Bera, and N. Mandal. "Design and analysis of flow measurement of conductive liquid and transmission via optical channel." *Flow Measurement and Instrumentation* 52 (2016): 246-254. <https://doi.org/10.1016/j.flowmeasinst.2016.11.003>
- [61] Ayliffe, H. Edward, and R. D. Rabbitt. "An electric impedance based microelectromechanical system flow sensor for ionic solutions." *Measurement Science and Technology* 14, no. 8 (2003): 1321. <https://doi.org/10.1088/0957-0233/14/8/318>
- [62] Rai, Purnima, and Upendra Mishra. "Numerical Simulation of Boundary Layer Flow Over a Moving Plate in The Presence of Magnetic Field and Slip Conditions." *Journal of Advanced Research in Fluid Mechanics and Thermal Sciences* 95, no. 2 (2022): 120-136. <https://doi.org/10.37934/arfmts.95.2.120136>
- [63] Urmi, Wajiha Tasnim, Md Mustafizur Rahman, Kumaran Kadirgama, Zetty Akhtar Abd Malek, and Wahaizad Safiei. "A Comprehensive Review on Thermal Conductivity and Viscosity of Nanofluids." *Journal of Advanced Research in Fluid Mechanics and Thermal Sciences* 91, no. 2 (2022): 15-40. <https://doi.org/10.37934/arfmts.91.2.1540>
- [64] Mopuri, Obulesu, Charankumar Ganteda, Bhagyashree Mahanta, and Giulio Lorenzini. "MHD heat and mass transfer steady flow of a convective fluid through a porous plate in the presence of multiple parameters." *Journal of Advanced Research in Fluid Mechanics and Thermal Sciences* 89, no. 2 (2022): 56-75. <https://doi.org/10.37934/arfmts.89.2.5675>
- [65] Yen, Wah Tey, Yutaka Asako, Nor Azwadi Che Sidik, and Goh Rui Zher. "Governing equations in computational fluid dynamics: Derivations and a recent review." *Progress in Energy and Environment* 1 (2017): 1-19.
- [66] Khan, Umair, William Pao, Nabihah Sallih, and Farruk Hassan. "Flow Regime Identification in Gas-Liquid Two-Phase Flow in Horizontal Pipe by Deep Learning." *Journal of Advanced Research in Applied Sciences and Engineering Technology* 27, no. 1 (2022): 86-91. <https://doi.org/10.37934/araset.27.1.8691>
- [67] Akaje, Wasiu, and B. I. Olajuwon. "Impacts of Nonlinear thermal radiation on a stagnation point of an aligned MHD Casson nanofluid flow with Thompson and Troian slip boundary condition." *Journal of Advanced Research in Experimental Fluid Mechanics and Heat Transfer* 6, no. 1 (2021): 1-15.
- [68] Sahri, Dzulkarnain Mohd, Nabilah Zaini, Noor Shawal Nasri, Husna Mohd Zain, Norhana Mohamed Rashid, and Anis Shahirah Noor Shawal. "Length and Diameter Ratio Effect on Gas Homogeneity Gradients Flow for Multi-Channel Carbon Filtration System Using Computational Fluid Dynamic Analysis." *Journal of Advanced Research in Applied Mechanics* 75, no. 1 (2020): 1-5. <https://doi.org/10.37934/aram.75.1.15>